

Water Soluble, Core-Modified Porphyrins. 3. Synthesis, Photophysical Properties, and in Vitro Studies of Photosensitization, Uptake, and Localization with Carboxylic Acid-Substituted Derivatives

Youngjae You,[†] Scott L. Gibson,[‡] Russell Hilf,[‡] Sherry R. Davies,[§] Allan R. Oseroff,[§] Indrajit Roy,[†] Tymish Y. Ohulchanskyy,[†] Earl J. Bergey,[†] and Michael R. Detty^{*,†}

Institute for Lasers, Photonics, and Biophotonics, Department of Chemistry, University at Buffalo, The State University of New York, Buffalo, New York 14260-3000, Department of Biochemistry and Biophysics, University of Rochester Medical Center, 601 Elmwood Avenue, Box 607, Rochester, New York 14642, and PDT Center, Roswell Park Cancer Institute, Elm and Carlton Streets, Buffalo, New York 14263

Received March 26, 2003

Water soluble, core-modified porphyrins **1–5** bearing 1–4 carboxylic acid groups were prepared and evaluated in vitro as photosensitizers for photodynamic therapy. The 21,23-core-modified porphyrins **1–5** gave band I absorption maxima with λ_{max} of 695–701 nm. The number of carboxylic acid groups in the dithiaporphyrins **1–4** had little effect on either absorption maxima (λ_{max} of 696–701 nm for band I) or quantum yields of singlet oxygen generation [$\phi(^1\text{O}_2)$ of 0.74–0.80]. Substituting two Se atoms for S gave a shorter band I absorption maximum (λ_{max} of 695 nm) and a smaller value for the quantum yield for generation of singlet oxygen [$\phi(^1\text{O}_2)$ of 0.30]. The phototoxicity of **1–5** was evaluated against R3230AC cells. The phototoxicities of dithiaporphyrin **2**, sulfonated thiaporphyrin **30**, HPPH, and Photofrin were also evaluated against Colo-26 cells in culture using 4 J cm⁻² of 570–800 nm light. Compound **2** was significantly more phototoxic than sulfonated dithiaporphyrin **30**, HPPH, or Photofrin. Cellular uptake was more greater for compounds **1**, **2**, and **5** relative to compounds **3** and **4**. Confocal scanning laser microscopy and double labeling experiments with rhodamine 123 suggested that the mitochondria were an important target for dithiaporphyrins **1** and **2**. Inhibition of mitochondrial cytochrome *c* oxidase activity in whole R3230AC cells was observed in the dark with compounds **1** and **30** and both in the dark and in the light with core-modified porphyrin **2**.

Introduction

Photodynamic therapy (PDT) has gained acceptance as a front line cancer therapy for a variety of malignancies.^{1–3} Regulatory agencies in the U.S.A., Japan, The Netherlands, Germany, France, and Great Britain have approved this treatment regimen for cancers of the lung, esophagus, genitourinary tract, and head and neck as well as other disease conditions such as actinic keratinitis and macular degeneration.^{3–8} The majority of the clinical trials and PDT protocols that have received approval utilized Photofrin, a complex derivative of hematoporphyrin, as the photosensitizer. While effective, Photofrin has several drawbacks that limit its general clinical use including minimal absorption in the red region of the visible spectrum where light penetration into tissue is maximal, long-term skin photosensitivity,⁹ loss of absorbance during irradiation due to rapid photobleaching, structural composition that does not easily allow chemical modification,¹⁰ and a lack of specificity for either target malignancies or intracellular sites.

The drawbacks associated with Photofrin have provided the impetus for the search for new photosensitizers with greater specificity and efficacy.^{3,11} Various

meso-substituents have been incorporated in the porphyrin molecule to give longer wavelength absorption maxima. Other variations of porphyrins and porphyrin-related molecules (chlorins and bacteriochlorins (Chart 2), texaphyrins, phthalocyanines) have been prepared and evaluated as photosensitizers for PDT.³ Chlorin and bacteriochlorin derivatives are the products of reduction of one or two pyrrole carbon–carbon double bonds, respectively. Texaphyrin derivatives incorporate five nitrogen atoms in the central core.

We have been investigating the photosensitizing properties of 5,10,15,20-tetraaryl-21,23-dithia, 21-selena-23-thia, and 21,23-diselenaporphyrins as a porphyrin variation with several desirable features.¹² These core-modified porphyrins can be synthesized in a pure form, have longer wavelengths of absorption than the corresponding porphyrin, and generate singlet oxygen with high quantum yields. Unlike any of the porphyrin, chlorin, bacteriochlorin, texaphyrin, or phthalocyanine derivatives, the 21,23-heteroatom contacts in the core-modified porphyrins are less than the sum of van der Waals' radii¹³ and the 21,23-core-modified porphyrins are no longer capable of binding a metal ion within the core and can only bind to metals that approach the heteroatoms from above or below the porphyrin core.¹⁴ This aspect of the core-modified porphyrins represents a significant difference from other porphyrin-related photosensitizers and should lead to novel pharmacokinetics and related biological properties.

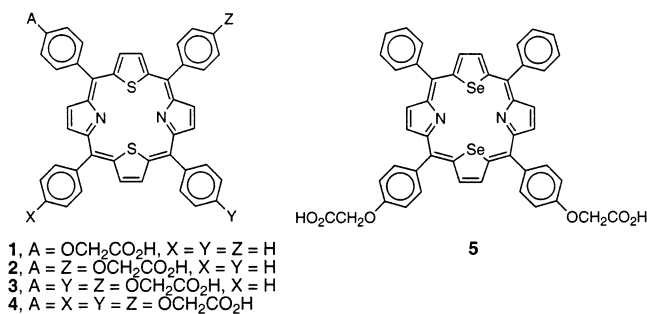
* To whom correspondence should be addressed. Tel: 716-645-6800. Fax: 716-645-6963. E-mail: mdetty@acsu.buffalo.edu.

[†] The State University of New York.

[‡] University of Rochester Medical Center.

[§] Roswell Park Cancer Institute.

Chart 1

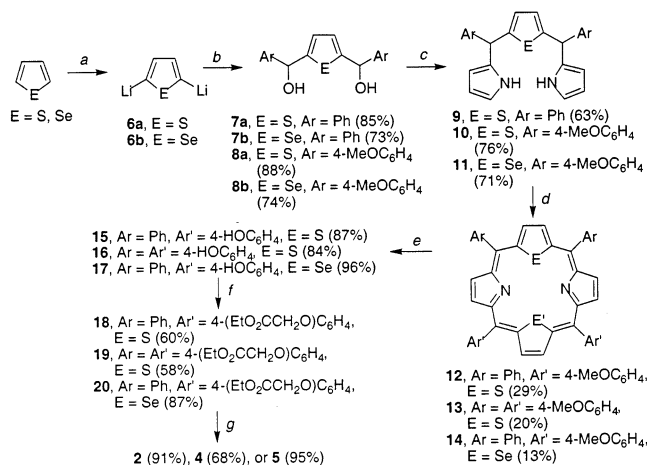


Our initial biological studies demonstrated that the core-modified porphyrins were potent photosensitizers with limited dark toxicity and minimal cutaneous phototoxicity.¹² Core-modified porphyrins with two 4-sulfonatophenyl substituents at the 5- and 10-*meso*-positions of the ring were more effective photosensitizers both in vitro and in vivo than core-modified porphyrins with four 4-sulfonatoaryl substituents at the 5-, 10-, 15-, and 20-positions of the porphyrin ring. Several core-modified porphyrins with two 4-sulfonatophenyl substituents were significantly more effective than Photofrin in vitro and, at 20-fold lower concentrations than Photofrin, were comparable to Photofrin in efficacy in vivo.^{12b}

The *pK_a* values of the sulfonato substituents described above are sufficiently low to keep the core-modified porphyrins anionic over the range of physiological pH. Replacing the sulfonato groups with carboxylic acid groups gives core-modified porphyrins that achieve both neutral and anionic states at physiological pH. For the study of carboxylate derivatives of the core-modified porphyrins, we have prepared 21,23-dithiaporphyrins **1–4** with 1–4 4-phenoxyacetic acid residues, respectively, in the *meso*-positions and 21,23-diselenaporphyrin **5** with two 4-phenoxyacetic acid residues at the 5,10-*meso*-positions (Chart 1). Several physical properties of these compounds were investigated, including electronic absorption, quantum yields for the generation of singlet oxygen and for fluorescence, photobleaching, and lipophilicity. In general, the core modification of heteroatoms alters the photophysical properties significantly, while changes in the *meso*-groups affect the lipophilicity. To evaluate further the potential development of these core-modified porphyrins as therapeutics, a series of studies were performed in vitro to evaluate dark and phototoxicities, cellular uptake, and localization.

Results and Discussion

Chemistry. Synthesis of Dicarboxylic Acids 2 and 5 and Tetracarboxylic Acid 4. The synthesis of compounds **2**, **4**, and **5** with an even number of carboxylic acid groups is shown in Scheme 1 and follows our previous synthetic strategy.¹² 2,5-Dilithiochalcogenophenes **6**¹³ were added to benzaldehyde to give 2,5-di(phenylhydroxymethyl)chalcogenophenes **7a,b**¹² and *p*-methoxybenzaldehyde to give chalcogenophenes **8a**^{12b} and **8b**. Diols **7a** and **8** were converted to the corresponding 2,5-di(arylpyrrolomethyl)chalcogenophenes **9–11** with pyrrole and BF₃-etherate. Diol **7a** was condensed with thiophene **10** in the presence of tetrachlorobenzoquinone (TCBQ) and *p*-toluenesulfonic acid (TsOH) in CH₂Cl₂ to give 21,23-dithiaporphyrin **12** in

Scheme 1. Synthesis of Core-Modified Porphyrins **2**, **4**, and **5**^a

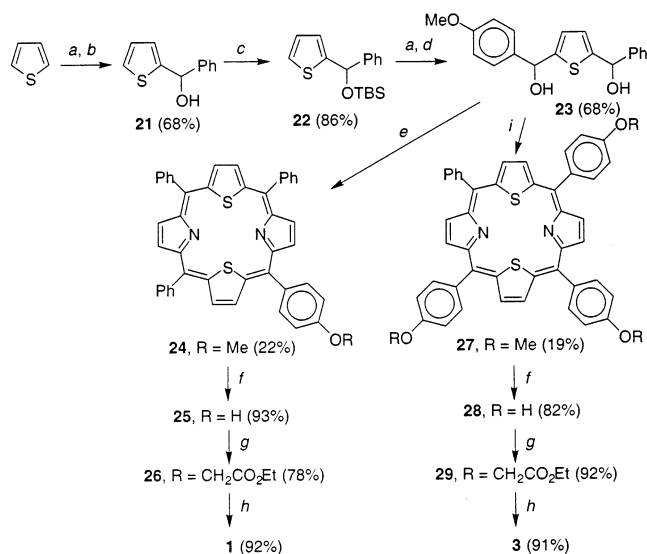
^a Key: (a) 2.5 equiv of BuLi, TMEDA, hexanes, 23 °C to reflux. (b) PhCH=O or 4-MeOC₆H₄CH=O. (c) BF₃, pyrrole. (d) **7** or **8**, TCBQ, TsOH, CH₂Cl₂. (e) BBr₃, CH₂Cl₂. (f) BrCH₂CO₂Et, K₂CO₃, acetone. (g) NaOH, aqueous THF.

29% isolated yield (Scheme 1). Similarly, diol **8a** and **10** gave dithiaporphyrin **13** in 20% isolated yield and diol **7b** and selenophene **11** gave 21,23-diselenaporphyrin **14** in 13% isolated yield. The demethylation of **12–14** with BBr₃ in CH₂Cl₂ gave phenolic core-modified porphyrins **15–17**, which were alkylated with ethyl bromoacetate and K₂CO₃ in acetone to give **18–20**. The ester functional groups of **18–20** were saponified with NaOH in aqueous tetrahydrofuran (THF) to give dicarboxylic acid derivatives **2** and **5** and tetracarboxylic acid derivative **4**.

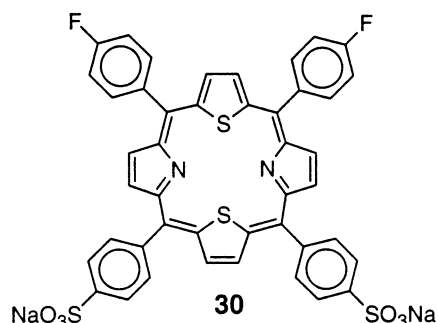
Synthesis of Monocarboxylic Acid 1 and Tricarboxylic Acid 3. The critical step in the synthesis of core-modified porphyrins with an odd number of phenoxyacetic acid residues is breaking the symmetry of the 2,5-di(arylhydroxymethyl)thiophenes as shown in Scheme 2. Treating thiophene with a limiting amount of BuLi gives 2-lithiothiophene, which reacts with benzaldehyde to give 2-(1-phenyl-1-hydroxymethyl)thiophene (**21**) in 68% isolated yield.¹⁵ Compound **21** was then protected as the TBS ether to give **22**, which was then lithiated with BuLi. The resulting 5-lithiothiophene was treated with *p*-methoxybenzaldehyde to give **23**, which is a common intermediate for the synthesis of **1** and **3**, following removal of the TBS protecting group.

The condensation of thiophene **9**^{12b} and diol **23** with TsOH and TCBQ in CH₂Cl₂ gave methoxyphenyl dithiaporphyrin **24** in 22% isolated yield. Demethylation with BBr₃ gave **25**, which was alkylated with ethyl bromoacetate to give ester **26**. Saponification with NaOH in aqueous THF gave monocarboxylic acid **1**. Similarly, condensation of thiophene **10**^{12b} and diol **23** gave tris(methoxyphenyl)dithiaporphyrin **27** in 22% isolated yield, which was then demethylated with BBr₃ to give trisphenol **28**. Compound **28** was then alkylated with ethyl bromoacetate to give triester **29**, which was saponified with NaOH in aqueous THF to give tricarboxylic acid **3**.

Electronic Absorption Spectra of Core-Modified Porphyrins 1–5. 21- and 21,23-Core-modified porphyrins absorb light of longer wavelengths than the corre-

Scheme 2. Synthesis of Core-Modified Porphyrins 1 and 3^a


^a Key: (a) 1 equiv of BuLi, TMEDA, hexanes, 0 °C. (b) PhCH=O. (c) TBSCl, Et₃N. (d) (i) 4-MeOC₆H₄CH=O; (ii) aqueous HCl. (e) **9**, TsOH, CH₂Cl₂. (f) BBr₃, CH₂Cl₂. (g) BrCH₂CO₂Et, K₂CO₃, acetone. (h) NaOH, aqueous THF. (i) **10**, TsOH, CH₂Cl₂.

Chart 2


sponding porphyrins. For core-modified porphyrins **1–5** and bis-4-sulfonatophenyl-21,23-dithiaporphyrin **30** (Chart 2), which is an effective photosensitizer both in vitro and in vivo,^{12b} substituents on the aryl groups at the *meso*-positions appear to have little effect on the absorption maxima of the core-modified porphyrins.¹² Individual absorption spectra for **1–5** in MeOH are shown in Figures S1–S5 in the Supporting Information. For **1–4**, the band maxima for all bands move to slightly longer wavelengths as the number of carboxylic acid groups increases.

Replacing the core sulfur atoms of **2** with selenium atoms had a more pronounced effect than varying the number of carboxylic acid groups or other *meso*-substituents. The absorption maxima for bands III and IV and the solet band are at 13–15 nm longer wavelengths for 21,23-diselenaporphyrin **5** relative to 21,23-dithiaporphyrin **2** while maxima for bands I and II are at 3–4 nm shorter wavelengths relative to **2**.

Singlet Oxygen Generation. The photochemical production of singlet oxygen is thought to be the primary mechanism for cytotoxicity for PDT with many photosensitizers.^{1–3,10} One measure of a photosensitizer's potential is the efficiency of singlet oxygen generation as measured by $\phi(^1O_2)$. It has been observed that 5,10,15,20-tetraarylporphyrins and 21-thiaporphyrins with iden-

Table 1. UV–Vis Band Maxima and Molar Absorptivities for 1–5 and 30 in MeOH, λ_{max} nm ($\epsilon \times 10^{-3} M^{-1} cm^{-1}$)

compd	solet	band IV	band III	band II	band I
1	433 (241)	512 (18.7)	546 (6.2)	633 (1.8)	696 (3.7)
2	434 (234)	514 (21.6)	549 (9.9)	634 (1.7)	699 (5.6)
3	436 (275)	515 (22.9)	550 (10.2)	635 (1.8)	700 (5.7)
4	437 (178)	516 (12.0)	552 (7.1)	636 (2.2)	701 (4.2)
5	448 (147)	527 (17.2)	564 (3.4)	631 (1.7)	695 (2.8)
30	431 (476)	518 (15.7)	560 (8.3)	633 (2.3)	701 (4.6)

tical *meso*-substituents have similar values of $\phi(^1O_2)$ while 21,23-dithiaporphyrins have slightly smaller values of $\phi(^1O_2)$.¹² 21,23-Dithiaporphyrin **30** is an effective photosensitizer both in vitro and in vivo with $\phi(^1O_2) = 0.74$ in MeOH at 25 °C.^{12b}

Values of $\phi(^1O_2)$ for dithiaporphyrins **1–5** were determined by direct methods¹⁶ using dithiaporphyrin **30**^{12b} as a standard. As shown in Figure S6 of the Supporting Information, the luminescence intensities from singlet oxygen generated by irradiation of MeOH solutions of **1–4** and **30** at ambient temperature with identical absorbance at 532 nm (Figure S7, Supporting Information) were essentially identical from all five solutions. Values of $\phi(^1O_2)$ for **1–4** were between 0.74 and 0.80 with $\phi(^1O_2)$ for **30** of 0.74 (Table 2). The diselenaporphyrin **5** was less efficient at generating ¹O₂ (Figure S8, Supporting Information) with $\phi(^1O_2)$ of 0.30.

Photobleaching of 21,23-Core-Modified Porphyrins 1–5. Although core-modified porphyrins **1–5** and **30** appeared to be photostable to 532 nm irradiation in air-saturated MeOH for at least 20–30 min, broadband irradiation in pH 7.4 phosphate-buffered saline (PBS) gave some photobleaching. Rates of photobleaching of core-modified porphyrins **1–5** and **30** as well as the rate of photobleaching of Photofrin in 0.05 M, pH 7.4, PBS were determined under irradiation with 200 mW cm⁻² of broadband 350–750 nm white light emitted from a focused and filtered 750 W tungsten source. Concentrations ($\approx 5 \times 10^{-6}$ M) were adjusted such that the initial absorbance of the solet band was ≈ 1.0 in a 1 cm cell. 21,23-Diselenaporphyrin **5** was the most photostable of the five compounds examined with a rate of loss of $<3 \times 10^{-6} s^{-1}$ under these conditions (Table 2). Compounds **1**, **2**, and **30** have comparable photostability with a rate of loss of $1.26 \times 10^{-4} s^{-1}$ for **2**, $1.60 \times 10^{-4} s^{-1}$ for **1**, and $1.90 \times 10^{-4} s^{-1}$ for **30** (Table 2). Compound **2** was a factor of 4.5 times more stable than Photofrin, which had a rate of loss of $5.69 \times 10^{-4} s^{-1}$. 21,23-Dithiaporphyrins **3** and **4** were the least photostable compounds of the series with rates of loss of 6.77×10^{-4} and $1.00 \times 10^{-3} s^{-1}$, respectively (Table 2).

***n*-Octanol/Water Partition Coefficients.** The octanol/water partition coefficients for **1–5** and **30** were all measured with pH 7.4 PBS (0.05 M) as the aqueous phase using UV–visible spectrometry (Table 2). The measurements were done using a “shake flask” direct measurement, and results are the average of three independent measurements.¹⁷ Compound **1** with one carboxylic acid was the most lipophilic with $\log P > 3.5$. $\log P$ values for dithiaporphyrin **2** and diselenaporphyrin **5** with two carboxylic acids were determined to be 0.036 and -0.67 , respectively. Replacing the two S atoms of **2** with the two Se atoms of **5** gave a -0.7 change in $\log P$, which is consistent with our observations in chalcogenopyrylium dyes where replacing one

Table 2. Quantum Yields for the Generation of Singlet Oxygen [$\phi(^1O_2)$], Rates of Photobleaching (k_{PB}) with Broadband Light, *n*-Octanol/Water Partition Coefficients ($\log P$), Emission Maxima (λ_{EM}), and Quantum Yields for Fluorescence (ϕ_F) for Core-Modified Porphyrins **1–5** and **30**

compd ^a	$\phi(^1O_2)$	$k_{PB} \times 10^4$ (s ⁻¹)	$\log P$	λ_{EM} (nm) ^c	ϕ_F^c
1	0.78 ± 0.03	1.26 ± 0.09	>3.5	710	0.004 ± 0.001
2	0.80 ± 0.03	1.60 ± 0.05	0.036 ± 0.005	710	0.007 ± 0.001
3	0.74 ± 0.03	6.77 ± 0.08	-1.49 ± 0.05	710	0.008 ± 0.001
4	0.78 ± 0.03	10.0 ± 0.4	-0.95 ± 0.08	712	0.008 ± 0.001
5	0.30 ± 0.03	<3 × 10 ⁻²	-0.67 ± 0.04		<0.001
30	0.74 ^b	1.90 ± 0.04	-1.9 ± 0.1	710	0.004 ± 0.001

^a Value ± standard deviation. ^b Ref 12b. ^c In MeOH.

S atom with one Se atom led to a 0.1–0.3 more negative value of $\log P$.¹⁸ Compounds **3** and **4** were much more hydrophilic with values of $\log P$ of -1.49 ± 0.05 and -0.95 ± 0.08 , respectively. Compound **30** with two sulfonate groups was the most hydrophilic compound with a $\log P$ of -1.9 ± 0.1 .

Quantum Yields for Fluorescence. Dithiaporphyrins **1–4** were emissive although quantum yields for fluorescence (ϕ_F) were low (Table 2). The quantum yield standard used in these studies was a freshly prepared solution of Rhodamine 6G ($\phi_F = 1.0$) dissolved in MeOH. A small (≤ 15 nm) Stokes shift was observed for the core-modified porphyrins **1–4**, and values of ϕ_F were between 0.003 and 0.008. Selenium-containing core-modified porphyrin **5** was nonemissive.

Summary of Physical Properties. Substituent changes in the *meso*-aryl groups of core-modified porphyrins have little impact on absorption spectra and quantum yields for the generation of singlet oxygen and fluorescence. Compounds **1–4** and **30** all have band I maxima near 700 nm and values of $\phi(^1O_2)$ between 0.74 and 0.80. Heteroatom changes have a much greater impact. The substitution of two Se atoms for the two S atoms of **2** gives compound **5**. The two Se atoms are much less than van der Waals' radii apart distorting the planarity of the core-modified porphyrin ring,¹² which leads to slight spectral differences from **1–4** and to smaller values of $\phi(^1O_2)$ and ϕ_F . Compound **5** has greater photostability than compounds **1–4** and **30**, and compounds **1**, **2**, **5**, and **30** all have significantly greater photostability than Photofrin with respect to broadband irradiation. The number and identity of the water-solubilizing functionality on *meso*-aryl groups have its greatest impact on values of $\log P$.

Biology. While a successful photosensitizer will have certain desirable physical and photophysical properties, the viability of a photosensitizer as a functioning drug will depend on adsorption, distribution, metabolism, and excretion (ADME) properties.¹⁹ As a starting point to evaluate biological properties, we examined compounds **1–5** in vitro using R3230AC rat mammary adenocarcinoma cells to establish dark and phototoxicity, cellular uptake, and sites of localization.

Dark and Phototoxicities In Vitro. One very desirable property for new photosensitizers is high phototoxicity with minimal or no dark toxicity. Cultured R3230AC cells were incubated for 24 h in the dark with various concentrations of photosensitizer and were then washed and irradiated with broadband light (350–750 nm) delivered at 1.4 mW cm⁻² for 1 h (5 J cm⁻²). Light-treated cells and dark controls were subsequently incubated for 24 h, and cell survival was determined.

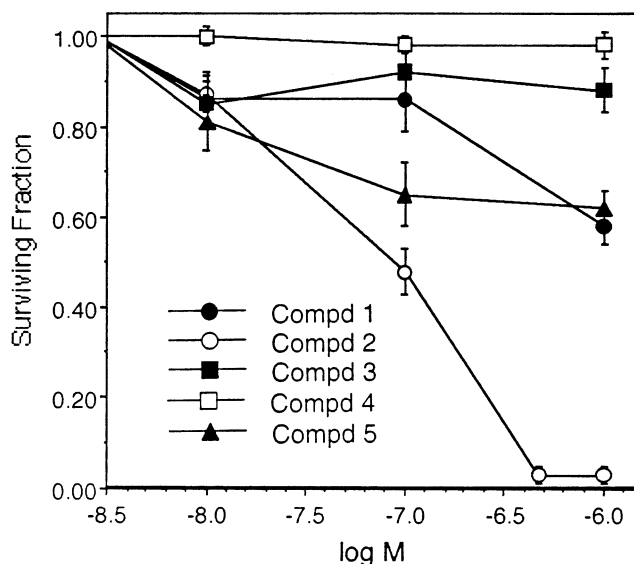


Figure 1. Cell viability of cultured R3230AC cells after photosensitization in the presence of core-modified porphyrins **1–5**. Data are expressed as the percent survival of viable cells relative to untreated controls following treatment with various concentrations of **1–5** (1×10^{-8} to 1×10^{-6} M) and broadband light (350–750 nm) delivered at 1.4 mW cm⁻² from a filtered 750 W tungsten source for a total of 5.0 J cm⁻². Each data point represents the mean surviving fraction of viable cells calculated from at least three separate experiments performed in duplicate; bars are the SEM.

None of the core-modified porphyrins **1–5** displayed any significant dark toxicity at concentrations $\leq 1 \times 10^{-6}$ M (Figures S9–S13, Supporting Information). In addition, dithiaporphyrins **3** and **4** with three and four carboxylic acid residues, respectively, showed little phototoxicity upon irradiation (Figure 1). In contrast, dithiaporphyrin **1** (1×10^{-6} M) showed significant cell phototoxicity ($P < 0.005$) as compared to cells maintained in the dark for the same 24 h period with 1×10^{-6} M **1**. Irradiation of cultures in the presence of 1×10^{-7} or 1×10^{-8} M **1** did not result in any significant decrease in cell viability as compared to nonirradiated controls or cells exposed to the same concentrations of **1** in the dark over the same time period.

The data presented in Figure 1 demonstrate that dithiaporphyrin **2** was significantly more phototoxic than **1**. At 1×10^{-7} M, **2** combined with irradiation resulted in a 53% loss in cell viability while **1** under the same conditions induced no significant reduction in cell numbers, a significant difference of $P < 0.001$ when the phototoxic effects of the two core-modified porphyrins were compared. At 1×10^{-6} M, dithiaporphyrin **1** reduced cell viability by 41% 24 h after irradiation, but

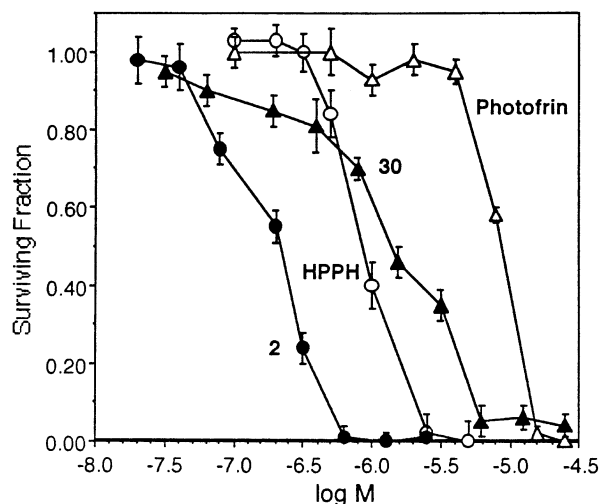


Figure 2. Cell viability of cultured Colo-26 cells after photosensitization in the presence of core-modified porphyrins **2** and **30**, HPPH, and Photofrin. Data are expressed as the surviving fraction of viable cells relative to untreated controls following treatment with various concentrations of **2**, **30**, HPPH, and Photofrin and filtered 590–800 nm light at 37 °C with 14 mW cm⁻² for a total light dose of 4 J cm⁻².

irradiation of cells treated with core-modified porphyrin **2** gave a 96% reduction in cell viability, resulting in a significant difference in phototoxicity of $P < 0.001$.

Cells treated with diselenaporphyrin **5** and light showed some phototoxicity as compared to that observed in dark controls when **5** was present in cell cultures at 1×10^{-8} to 1×10^{-6} M. However, the phototoxicity of **5** was significantly less than that observed for core-modified porphyrin **2** ($P < 0.001$, Figure 1).

A Comparison of Dithiaporphyrin 2 with 30, HPPH, and Photofrin. Compound **2** was significantly more phototoxic than compounds **1** or **3–5**. Comparison of the phototoxicity of **2** with **30**, Photofrin, and HPPH, a pyropheophorbide derivative currently in clinical trials,^{11a} is presented in Figure 2. These experiments were carried out with cultured Colo-26 cells, a murine colon carcinoma cell line. Cells were incubated for 24 h in the dark with various concentrations of sensitizer and were then washed prior to treatment with filtered 590–800 nm light delivered at 14 mW cm⁻² for a total light dose of 4 J cm⁻². Light-treated cells and dark controls were then incubated for 24 h, and cell survival was determined. Results are compiled in Figure 2. No significant dark toxicity was observed at concentrations $< 10^{-4}$ M. The concentration of Photofrin that gave a 50% cell kill under these conditions was approximately 10 μ M, 1 μ M for compound **30** and HPPH, and 0.1 μ M for compound **2**. In this comparison, compound **2** was significantly ($P < 0.001$) more phototoxic than **30**, HPPH, or Photofrin.

Uptake of Core-Modified Porphyrins 1–5 into Cultured R3230AC Cells. As shown in Figure 1, the number of carboxylic acid residues and the 21,23-heteroatoms has an impact on the efficacy of **1–5**. Two likely consequences of structural changes are changes in cellular uptake or cellular localization. The uptake of core-modified porphyrins **1–5** was determined by fluorescence for compounds **1–4** and by absorbance for compound **5**. Following the incubation periods in the presence of **1–5**, cells were washed, detached, and

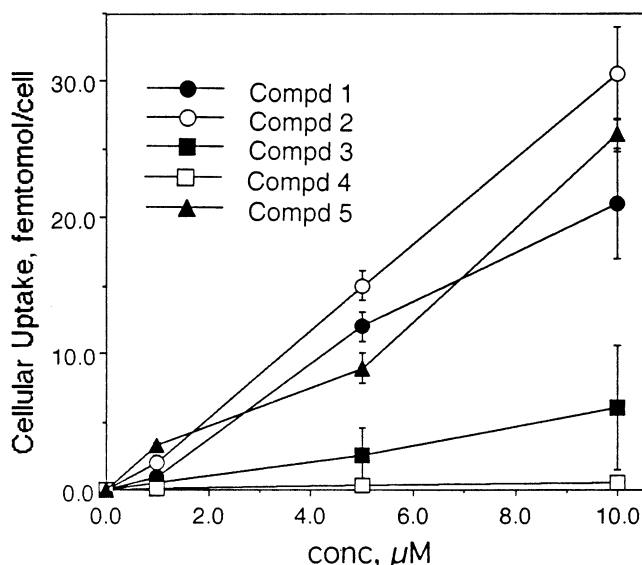


Figure 3. Cellular uptake of core-modified porphyrins **1–5** in cultured R3230AC rat mammary adenocarcinoma cells. Cells were incubated with 1×10^{-6} , 5×10^{-6} , and 1×10^{-5} M concentrations of **1–5** for 3 h. After the incubation period, cells were washed, detached, and dissolved in 25% Scintigest. The intracellular fluorescence for **1–4** or the absorbance for **5** was compared to standard curves, and the data are presented as femtomoles of **1–5** per cell.

digested in 25% Scintigest. The fluorescence or absorbance values from the resulting solutions were compared to measurements from known concentrations of **1–5**. For compounds **1–4**, the fluorescence peak at 712 nm was measured following excitation at 440 nm. Spin-orbit effects from the two Se atoms of **5** effectively eliminated fluorescence in solutions of this molecule, and cellular uptake was determined by the absorbance at 440 nm. The data in Figure 3 depict the amount of core-modified porphyrins **1–5**, expressed as fmol/cell, measured intracellularly 3 h after exposure of R3230AC cells in culture to various concentrations of **1–5**. Core-modified porphyrin uptake reached a plateau after 3 h, and intracellular concentrations remained fairly constant over 24 h.

Cellular uptake was significantly greater for core-modified porphyrins **1**, **2**, and **5** relative to core-modified porphyrins **3** and **4**. Following incubation in media containing 5×10^{-6} M core-modified porphyrin, the intracellular concentrations of **1**, **2**, and **5** are 12 ± 0.8 , 15 ± 1 , and 8.9 ± 1.5 fmol/cell, respectively, at 3 h after exposure. In contrast, the intracellular concentration of **3** was 2.5 ± 2.0 fmol/cell 3 h following incubation with 5×10^{-6} M **3**. Core-modified porphyrin **4** was not detectable in cells at concentrations $\leq 5 \times 10^{-5}$ M (< 0.3 fmol/cell), and at 1×10^{-4} M, **4** was measured at 1.0 ± 0.5 fmol/cell.

Subcellular Targets. Mitochondrial Cytochrome c Oxidase Activity in Whole Cells. The subcellular localization of a photosensitizer can impact both dark and phototoxicity. For lipophilic porphyrin and porphyrin-related structures, accumulation of the photosensitizer occurs in the cellular membranes of organelles such as the mitochondria and lysosomes.²⁰ We examined the impact of carboxylated photosensitizers **1** and **2** and sulfonated dithiaporphyrin **30** on the mitochondria of R3230AC cells in culture both in the dark and in the

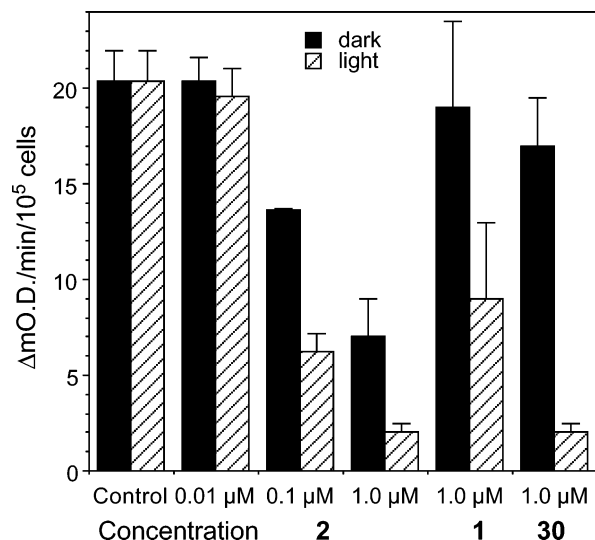


Figure 4. Effect of **1**, **2**, and **30** on mitochondrial cytochrome *c* oxidase activity in cultured whole R3230AC tumor cells in the dark and following irradiation. Cell culture and light exposure conditions are detailed in the Experimental Section. Columns represent the change in optical density (mOD) units per minute for 1×10^5 cells that were exposed to **1**, **2**, or **30** at indicated concentrations in the dark (solid columns) or 24 h after light exposure (striped columns). Each datum point represents the mean of at least three separate experiments performed in duplicate; the error bars are the SEM.

light by measuring the activity of cytochrome *c* oxidase. Cytochrome *c* oxidase is the terminal enzyme in the mitochondrial respiratory chain, and dark or photodamage either to this enzyme or to any preceding it in the respiration chain can lead to inhibition of cytochrome *c* oxidase activity.²¹

R3230AC cells were incubated with a 0.01–1.0 μM solution of **1**, **2**, or **30** for 24 h. Cell cultures were then washed and irradiated for 1 h with 350–750 nm light delivered at 1.4 mW cm^{-2} (5.0 J cm^{-2}). Both irradiated cells and photosensitizer-treated dark controls were then incubated for an additional 24 h in the dark at which time the activity of cytochrome *c* oxidase was determined (Figure 4). As shown in Figure 4, 1.0 μM solutions of **1** or **30** (as well as lower concentrations) had no impact on cytochrome *c* oxidase activity in nonirradiated R3230AC cells. In contrast, treating R3230AC cells with either 0.1 or 1.0 μM concentrations of **2** inhibited cytochrome *c* oxidase activity by 35 and 65%, respectively, in nonirradiated cells. Irradiation of the cells gave 55% inhibition of cytochrome *c* oxidase activity following treatment with 1.0 μM **1**, 70% inhibition following treatment with 0.1 μM **2**, 90% inhibition following treatment with 1.0 μM **2**, and 90% inhibition following treatment with 1.0 μM **30**.

As shown in Figure 4, mitochondrial cytochrome *c* oxidase activity in whole cells treated with **2** was inhibited both in the dark and following irradiation relative to control cells. These data are consistent with initial localization in the mitochondria of R3230AC cells in the absence of light and with further mitochondrial damage upon irradiation of photosensitizer-treated cells. In contrast, no significant inhibition of cytochrome *c* oxidase activity was observed in either **1**- or **30**-treated dark controls while 55 and 90% inhibition, respectively, were observed following irradiation of cells treated with

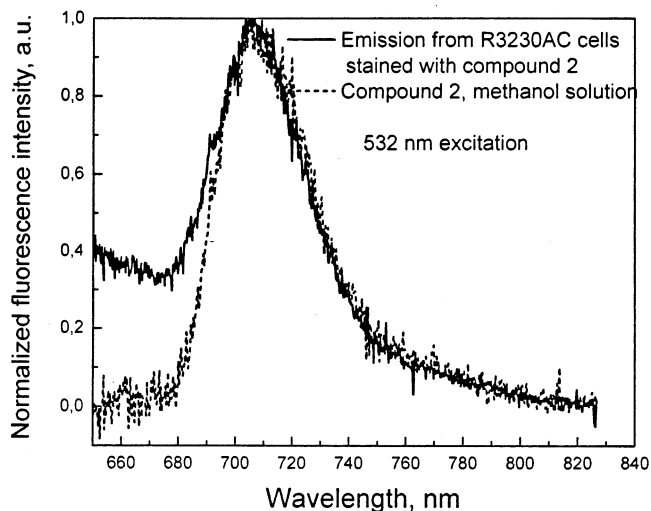


Figure 5. Spectrofluorometry of the emission from R3230AC cells treated with 2 μM dithiaporphyrins **2** and a solution of compound **2** in MeOH.

1.0 μM photosensitizer. Either compounds **1** and **30** are much less toxic toward mitochondria than **2** (i.e., not localized near a sensitive intramitochondrial site) or these photosensitizers do not localize initially in the mitochondria, but the photosensitizer may relocate to the mitochondria during irradiation.²²

Intracellular Localization of Core-Modified Porphyrins 1, 2, and 30 via Confocal Laser Scanning Microscopy. Confocal laser scanning microscopy (CLSM) is a powerful technique for visualizing a fluorescent photosensitizer within a cell, and when an organelle specific dye is employed along with the photosensitizer, dual label confocal microscopy can be used to image both the organelle specific dye and the photosensitizer in the same cell.²³ We examined the localization of dithiaporphyrins **1–4** and **30** in cells and used rhodamine 123 (Rh-123) to identify mitochondria intracellularly.²⁴

Untreated R3230AC cells, as well as cells treated with 2–10 μM **3** or **4** for 3 h, displayed no detectable fluorescence. Although the fluorescence from **3** or **4** in solution is weak (Table 2), the lack of any cellular fluorescence is consistent with the low uptake of dithiaporphyrins **3** and **4** (Figure 3). In contrast, emission was apparent from R3230AC cells treated with 2 μM **1** or **2** for 3 h. At lower concentrations of **1** or **2**, no cellular fluorescence was observed, which is most likely due to the low values of ϕ_F for **1** and **2** (Table 2). Localized spectrofluorometry indicated that the emission from the R3230AC cells was identical to emission from MeOH solutions of **1** (Figure S14, Supporting Information) or **2** (Figure 5).

Fluorescence micrographs of R3230AC cells treated with 2 μM dithiaporphyrin **1**, **2**, or sulfonated dithiaporphyrin **30** are shown in Figure 6. Three different patterns of staining were observed. In each case, cells were treated with a 2 μM solution of photosensitizer in culture media and were then washed and covered with fresh media. For cells treated with **1**, the emission was granular and observed throughout the cell except in the nucleus (Figure 6a). For cells treated with **2**, the emission was very diffuse and was observed throughout the entire cell except in the nucleus (Figure 6b). For cells

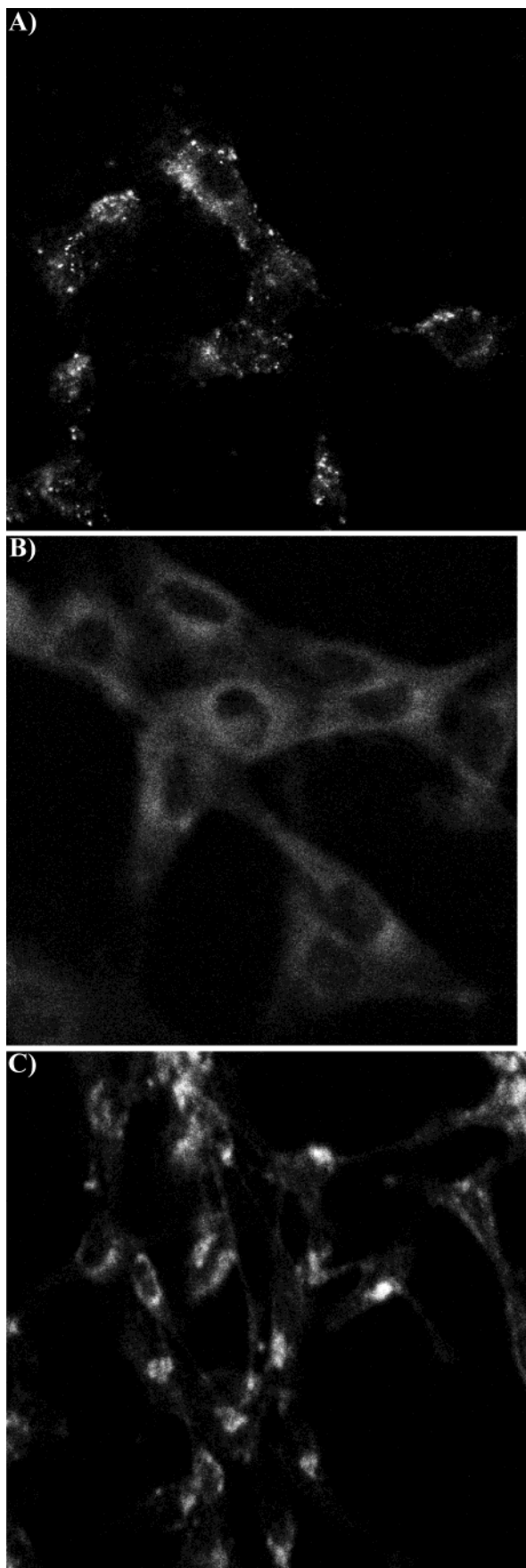


Figure 6. CSLM fluorescence images of R3230AC cells treated with (A) $2 \mu\text{M}$ **1**, (B) $2 \mu\text{M}$ **2**, and (C) $2 \mu\text{M}$ **30** for 3 h. Cell culture conditions and experimental details are detailed in the Experimental Section.

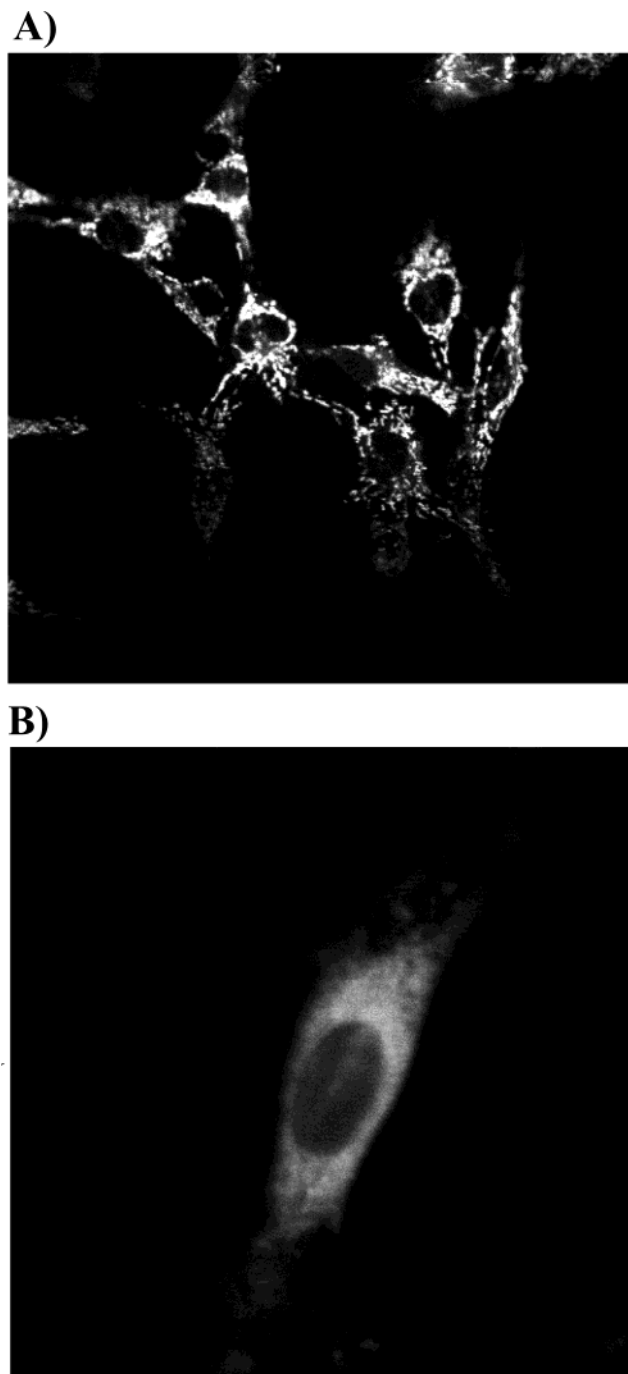


Figure 7. CSLM fluorescence images of R3230AC cells treated with (A) $1 \mu\text{M}$ Rh-123 for 20 min and (B) $2 \mu\text{M}$ **2** for 3 h followed by costaining with $1 \mu\text{M}$ Rh-123 for 20 min. Cell culture conditions and experimental details are detailed in the Experimental Section.

treated with sulfonated dithiaporphyrin **30**, the emission was localized near the nuclear membrane (Figure 6c).

The emission from cells treated with dithiaporphyrins **1**, **2**, and **30** can be compared with the emission from cells treated with Rh-123, a known mitochondrial stain, in Figure 7.²⁴ Emission from cells treated with a $1 \mu\text{M}$ solution of Rh-123 for 20 min was highly granular and similar to the emission observed from cells treated with dithiaporphyrin **1** (Figure 7a).

One problem with dual-labeling experiments with the dithiaporphyrins and Rh-123 is the difference in mag-

nitide of quantum yields for fluorescence for Rh-123 ($\lambda_{em} = 529$ nm, $\phi_F = 1.0$) and dithiaporphyrins **1**, **2**, and **30** ($\lambda_{em} = 710$ – 712 nm, $\phi_F = 0.004$ – 0.007). The strong emission from Rh-123 results in overlap of the tail of the emission from Rh-123 with the emission from the dithiaporphyrins. However, the primary emission from Rh-123 can be separated from the emission from the dithiaporphyrins using a 640 nm short-pass dichroic mirror. Most of the emission from Rh-123 is transmitted through the mirror while the emission from the core-modified porphyrins as well as the tail of the emission from Rh-123 is reflected orthogonally.

A fluorescence micrograph from emission collected through the dichroic mirror for R3230AC cells treated first with $2 \mu\text{M}$ **2** for 3 h, washed, treated with $1 \mu\text{M}$ Rh-123 for 20 min, washed, and covered with fresh media is shown in Figure 7b. In stark contrast to the granular fluorescence observed in cells treated only with Rh-123 in Figure 7a, the Rh-123 emission from cells treated with **2** and Rh-123 is diffuse throughout the cytoplasm. These data are consistent with disruption of the mitochondrial membrane potential by **2** or with exclusion of Rh-123 from the mitochondria in the presence of **2**.

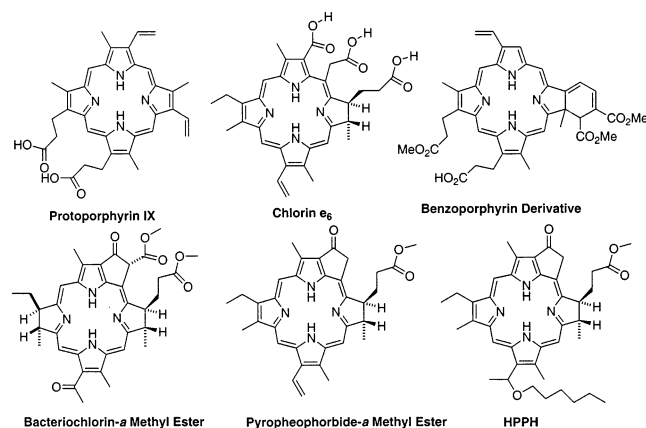
Summary and Conclusions

Sequential lithiation of thiophenes and selenophenes permits the preparation of 2,5-di-(1-hydroxymethyl)chalcogenophenes with two different substituents on the hydroxymethyl groups. When these derivatives are combined with symmetrical 2,5-di-(1-aryl-1-hydroxymethyl)chalcogenophenes, synthetic routes are now available to core-modified porphyrins with (i) one pair of identical, adjoining *meso*-substituents and two different *meso*-substituents, (ii) two adjoining pairs of identical *meso*-substituents, (iii) three identical *meso*-substituents, and (iv) four identical *meso*-substituents. The chalcogen atoms can be systematically varied as well to provide two S atoms, one S and one Se atom, or two Se atoms.^{12b} Systematic variation of structure is now possible with the core-modified porphyrins.

Photophysical properties are relatively insensitive to the number of carboxylic acid groups. However, replacing S atoms in the core with Se atoms, as in diselenaporphyrin **5**, results in diminished quantum yields for the generation of singlet oxygen and for fluorescence. In contrast, phototoxicity and cellular uptake were quite sensitive to the number of carboxylic acid residues in the *meso*-positions of compounds **1**–**5**. Compounds **3** and **4** display essentially no phototoxicity, which correlates with greatly reduced cellular uptake relative to **1**, **2**, and **5**. Of the three remaining compounds, dithiaporphyrin **2** with two carboxylic acid groups displays the greatest phototoxicity followed by dithiaporphyrin **1** with one carboxylic acid group and diselenaporphyrin **5** with two carboxylic acid groups. In a comparison of dithiaporphyrin **2** with sulfonated dithiaporphyrin **30**,^{12b} HPPH (Chart 3),^{11a} and Photofrin, dithiaporphyrin **2** displayed significantly greater phototoxicity (Figure 2). While dark toxicity as measured by cell viability did not appear to be an issue with compounds **1**–**5**, changes in the *meso*-substituents appear to impact site of localization (Figure 6) as well as mitochondrial function (Figures 4 and 7).

Most of the effective porphyrin-related photosensitizers^{3b} have a distinct hydrophobic end and a distinct

Chart 3



hydrophilic end as shown in the examples of Chart 3. Porphyrin derivatives with two polar groups on adjacent *meso*-positions provide more active photosensitizers than those with one, three, or four as determined by cell viability.²⁵ Sulfonated dithiaporphyrin **30** has two 4-sulfonatophenyl groups at the 5- and 10-positions with 4-fluorophenyl substituents at the 15- and 20-positions. Among the core-modified porphyrins **1**–**5**, the enhanced phototoxicity of compounds **1**, **2**, and **5** with hydrophobic and hydrophilic ends is reflected in increased cellular uptake of these core-modified porphyrins relative to compounds **3** and **4**.

The CLSM images from R3230AC cells treated with dithiaporphyrins **1** and **2** as well as the effects of compounds **1** and **2** on mitochondrial function strongly suggest that the mitochondria are an important target for these core-modified porphyrins. Many of the photosensitizers of Chart 2 also have the mitochondria as a significant target, and the similarities in structure suggest a common binding site. While a common binding site has yet to be ascertained, some possibilities include cytochrome *c* oxidase or an earlier enzyme in the respiratory chain, the peripheral benzodiazepine receptor (PBR) for which protoporphyrin IX and other porphyrins are natural ligands,²⁶ the antiapoptotic protein Bcl-2,²⁷ or some part of the complex that includes the PBR, Bcl-2, the voltage-dependent anion channel, the adenine nucleotide transporter, and the mitochondrial pore transition. The importance of binding to the PBR has been challenged in several studies.^{11a,28} One of these studies correlates increased phototoxicity of pyropheophorbide derivatives with enhanced lipophilicity rather than with PBR binding.^{11a} In contrast to those observations, the phototoxicity of dithiaporphyrin **2**, with $\log P = 0.036$, is much greater than dithiaporphyrin **1**, with $\log P > 3.5$.

At the molecular level, we are able to separate photophysical properties from lipophilicity through our choice of *meso* and core substituents. We have also demonstrated a correlation of uptake with phototoxicity as well as a correlation of uptake with lipophilicity. We are actively examining the correlation of structural features with subcellular localization.

Experimental Section

General Methods. Solvents and reagents were used as received from Sigma-Aldrich Chemical Co. (St. Louis, MO) unless otherwise noted. Cell culture medium was purchased

from GIBCO (Grand Island, NY). Fetal bovine serum (FBS) was obtained from Atlanta Biologicals (Atlanta, GA). Concentration in vacuo was performed on a Büchi rotary evaporator. NMR spectra were recorded at 23 °C on a Varian Gemini-300, Inova 400, or Inova 500 instrument with residual solvent signal as the internal standard: CDCl₃ (7.26 for proton, 77.16 for carbon). Infrared spectra were recorded on a Perkin-Elmer FT-IR instrument. UV-visible near-IR spectra were recorded on a Perkin-Elmer Lambda 12 spectrophotometer equipped with a circulating constant temperature bath for the sample chambers. Elemental analyses were conducted by Atlantic Microlabs, Inc. Q-TOF 2 electrospray mass spectrometry was conducted by the Campus Chemical Instrumentation Center of The Ohio State University (Columbus, OH). Compounds **13** and **20** were prepared as previously described in ref 12b.

Preparation of 2,5-Bis[1-(4-methoxyphenyl)hydroxymethyl]selenophene (8b). Selenophene (5.7 g, 43 mmol) was added to a solution of *n*-butyllithium (60 mL, 1.6 M in hexanes, 95 mmol) and *N,N,N,N*-tetramethylethylenediamine (TMEDA, 15 mL, 100 mmol) in 200 mL of hexanes, under an Ar atmosphere. The reaction mixture was heated at reflux for 2 h, cooled to ambient temperature, and transferred via a cannula to a pressure-equalizing addition funnel. This dilithioselenophene suspension was then added dropwise to a 0 °C solution of 4-methoxybenzaldehyde (11.2 g, 82 mmol) in anhydrous THF (200 mL), which had been degassed with Ar for 15 min. After the addition was complete, the mixture was warmed to ambient temperature, 300 mL of a 1 M solution of NH₄Cl was added, and the organic phase was separated. The aqueous phase was extracted with ether (3 × 300 mL). The combined organic extracts were washed with water (3 × 300 mL) and brine (300 mL), dried over MgSO₄, and concentrated to give a yellow oil. The crude product was precipitated by the slow addition of hexanes to an ether solution of **8b** to give 13.0 g (74%) of **8b** as a white solid; mp 90–92 °C. IR (KBr): 3400 (br), 2953, 1612, 1512 cm⁻¹. ¹H NMR (400 MHz, CDCl₃ + CD₃-OD): δ 3.78 (s, 6H), 4.44 (s, 2H), 5.31 (s, 2H), 6.76 (d, 2H, *J* = 4 Hz), 6.85 (d, 2H), 6.87 (d, 2H, *J* = 3 Hz), 7.27 (d, 2H, *J* = 3 Hz), 7.29 (d, 2H, *J* = 3 Hz). ¹³C NMR (75 MHz, 1:1 CDCl₃/CD₃OD): δ 54.95, 82.70, 113.64, 126.18, 127.97, 132.76, 153.64, 159.14. High-resolution Q-TOF MS: *m/z* 427.0429 (calcd for C₂₀H₂₀O₄⁸⁰Se + Na⁺, 427.0426).

Preparation of 2,5-Bis[1-(4-methoxyphenyl)-1-pyrrolo-methyl]selenophene (11). Compound **8b** (5.1 g, 13 mmol) was dissolved in excess pyrrole (35 mL), and the resulting solution was degassed with Ar. Boron trifluoride etherate was added (0.32 mL), and the resulting mixture was allowed to stir for 1 h at ambient temperature. The reaction was stopped by addition of CH₂Cl₂ (200 mL) followed by 40% NaOH (50 mL). The organic layer was separated, washed with water (3 × 200 mL) and brine (200 mL), dried over MgSO₄, and concentrated. The excess pyrrole was removed at reduced pressure at ambient temperature. The residual oil was purified via chromatography on SiO₂ eluted with 25% EtOAc/hexanes to give 4.5 g (71%) of **11** as a yellow oil. IR (neat): 3400 (br), 2957, 1610, 1510 cm⁻¹. ¹H NMR (500 MHz, CDCl₃): δ 3.82 (s, 6H), 5.57 (s, 2H), 5.99 (s, 2H), 6.18 (d, 2H, *J* = 2 Hz), 6.70 (s, 2H), 6.82 (s, 2H), 6.88 (AA', 4H, *J* = 8 Hz), 7.22 (BB', 4H, *J* = 8 Hz), 7.96 (br s, 2H). ¹³C NMR (75 MHz, CDCl₃): δ 47.41, 55.36, 107.40, 108.38, 114.04, 117.21, 127.34, 129.47, 133.82, 135.53, 154.09. High-resolution Q-TOF MS: *m/z* 525.1062 (calcd for C₂₈H₂₆N₂O₂⁸⁰Se + Na⁺, 525.1059).

Preparation of 2-[1-Phenyl-1-(*tert*-butyldimethylsilyloxy)methyl]thiophene (22). A mixture of 2-(1-phenyl-1-hydroxymethyl)thiophene, (4 g, 0.021 mol), which was prepared according to ref 15, TBSCl (9.5 g, 0.063 mol), DMAP (2.6 g, 0.021 mol), and Et₃N (3.7 mL, 0.063 mol) in 100 mL of dry CH₂Cl₂ was stirred at 0 °C for 2 h and was then warmed to ambient temperature for 24 h. The reaction mixture was partitioned between 400 mL of ether and 400 mL of saturated aqueous NaHCO₃. The organic layer was washed with water (3 × 400 mL) and brine (400 mL), dried over MgSO₄, and concentrated to give a yellow oil. Chromatography on SiO₂ eluted with 5% EtOAc/hexanes gave 5.5 g (86%) of **22** as a

colorless oil. ¹H NMR (400 MHz, CDCl₃): δ -0.02 (s, 3H), 0.05 (s, 3H), 0.93 (s, 9H), 5.97 (s, 1H), 6.74 (d, 1H, *J* = 3 Hz), 6.87 (dd, 1H, *J* = 5, 3 Hz), 7.18 (d, 1H, *J* = 5 Hz), 7.24 (dd, 1H, *J* = 7, 6 Hz), 7.32 (dd, 2H, *J* = 7, 7 Hz), 7.41 (d, 2H, *J* = 7 Hz). ¹³C NMR (75 MHz, CDCl₃): δ -4.89, -4.68, 18.45, 25.92, 73.31, 123.69, 124.70, 126.33, 126.47, 127.57, 128.38, 144.54, 150.58. High-resolution Q-TOF MS: *m/z* 327.1191 (calcd for C₁₇H₂₄-OSSi + Na⁺, 327.1215).

Preparation of 2-[1-(4-Methoxyphenyl)-1-hydroxymethyl]-5-(1-phenyl-1-hydroxymethyl)thiophene (23). Compound **22** (10.7 g, 35 mmol) was added to a solution of *n*-butyllithium (23 mL, 1.6 M in hexanes, 37 mmol) and TMEDA (5.8 mL, 38 mmol) in 150 mL of hexanes under an Ar atmosphere. The reaction mixture was stirred at ambient temperature for 30 min and was transferred via cannula to a pressure-equalizing addition funnel. The suspension of 2 lithio-**22** was then added dropwise to a 0 °C solution of 4-methoxybenzaldehyde (5.1 mL, 33 mmol) in anhydrous THF (150 mL), which had been degassed with Ar for 15 min. After addition was complete, the mixture was allowed to warm to ambient temperature, 300 mL of a 1 M solution of NH₄Cl was added, and the organic phase was separated. The aqueous phase was extracted with ether (3 × 300 mL). The combined organic extracts were washed with water (3 × 300 mL) and brine (300 mL), dried over MgSO₄, and concentrated to give a yellow oil. The oil was dissolved in a 1 M solution of Bu₄NF in THF (95 mL, 95 mmol) and stirred at ambient temperature for 1 h at which point 100 mL of saturated aqueous NH₄Cl was added. The resulting mixture was extracted with ether (4 × 100 mL). The combined organic extracts were washed with water (3 × 400 mL) and brine (400 mL), dried over MgSO₄, and concentrated. The crude diol was purified by column chromatography on SiO₂ eluted with 25% EtOAc/hexanes to give 7.8 g (68%) of predominantly one diastereomer of **23** as a yellow solid; mp 73–75 °C. IR (KBr): 3397 (br), 1511, 1161 cm⁻¹. ¹H NMR (400 MHz, CDCl₃): δ 2.62 (br s, 2H), 3.79 (s, 3H), 5.87 (s, 1H), 5.92 (s, 1H), 6.67 (s, 2H), 6.86 (d, 2H, *J* = 8.4 Hz), 7.32 (m, 5H), 7.40 (d, 2H, *J* = 7.6 Hz). ¹³C NMR (75 MHz, CDCl₃): δ 55.40, 72.29, 72.62, 114.00, 124.36, 124.58, 126.37, 126.40, 127.73, 127.78, 128.08, 128.62, 135.33, 143.01, 148.08, 148.67, 159.44. High-resolution Q-TOF MS: *m/z* 349.0874 (calcd for C₁₉H₁₈O₃S + Na⁺, 349.0875).

General Procedure for the Preparation of Porphyrins 12–14, 24, and 27. **Preparation of 5-(4-Methoxyphenyl)-10,15,20-triphenyl-21,23-dithiaporphyrin (24).** Compound **23** (3.0 g, 10 mmol), **9** (4.3 g, 10 mmol), and TCBQ (9.8 g, 40 mmol) were dissolved in 600 mL of CH₂Cl₂ that had been degassed under a stream of Ar bubbles for 20 min. TsOH monohydrate (1.9 g, 10 mmol) was added, and the reaction mixture was stirred for 0.5 h at ambient temperature. The reaction vessel was covered with aluminum foil, and the reaction mixture was heated at reflux for 1 h. The reaction mixture was concentrated, and the residue was redissolved in minimal CH₂Cl₂. The crude product was purified via chromatography on basic alumina eluted with CH₂Cl₂. Porphyrin **24** was isolated as the first red band. The crude product was washed with acetone and was then recrystallized from CH₂Cl₂/MeOH to give 1.5 g (22%) of **24** as a purple solid; mp > 300 °C. ¹H NMR (400 MHz, CDCl₃): δ 4.11 (s, 3H), 7.36 (d, 2H, *J* = 8.4 Hz), 7.81 (s, 9H), 8.18 (d, 2H, *J* = 8.4 Hz), 8.26 (d, 6H, *J* = 5.6 Hz), 8.69 (s, 3H, s), 8.72 (d, 1H, *J* = 4.4 Hz), 9.69 (s, 3H), 9.73 (d, 1H, *J* = 4.8 Hz). ¹³C NMR (75 MHz, CDCl₃): δ 55.75, 113.21, 127.56, 128.16, 133.81, 134.00, 134.10, 134.17, 134.27, 134.58, 134.61, 134.70, 135.48, 135.57, 135.65, 141.44, 147.83, 147.99, 148.03, 148.25, 156.48, 156.63, 156.89, 159.92. High-resolution Q-TOF MS: *m/z* 679.186 (calcd for C₄₅H₃₀N₂-OS₂ + H, 679.1878).

Preparation of 5,10-Bis-4-methoxyphenyl-15,20-diphenyl-21,23-dithiaporphyrin (12). 2,5-Bis[1-(phenyl-1-hydroxymethyl)thiophene]¹² (**9**, 1.42 g, 3.6 mmol) and 2,5-bis[1-(4-methoxyphenyl)-1-hydroxymethyl]thiophene^{12b} (**8a**, 1.28 g, 3.6 mmol) in 1 L of CH₂Cl₂ were treated with TCBQ (4.40 g, 18 mmol) and TsOH (0.76 g, 4.0 mmol) as described. The crude product was recrystallized from CH₂Cl₂/MeOH to give 0.75 g

(29% of **12** as a purple solid; mp > 300 °C. ¹H NMR (CDCl₃, 300 MHz): δ 4.07 (s, 6H), 7.34 (BB', 4H, *J* = 8.1 Hz), 7.79 (m, 6H), 8.17 (AA', 4H, *J* = 8.1 Hz), 8.24 (m, 4H), 8.67 (d, 2H, *J* = 4.5 Hz), 8.71 (d, 2H, *J* = 4.5 Hz), 9.67 (s, 2H), 9.72 (s, 2H). ¹³C NMR (CDCl₃, 75 MHz): δ 55.56, 113.03, 127.40, 127.97, 133.69, 133.79, 134.00, 134.16, 134.35, 134.56, 135.31, 135.40, 141.30, 147.68, 148.15, 156.38, 156.65, 159.75. High-resolution Q-TOF MS: *m/z* 677.2094 (calcd for C₄₆H₃₂N₂S₂ + H, 677.2085).

Preparation of 5,10-Bis(4-methoxyphenyl)-15,20-diphenyl-21,23-dithiaporphyrin (14). 2,5-Bis[1-(4-methoxyphenyl)-pyrrolomethyl]selenophene (**11**, 3.8 g, 7.6 mmol) and diol **7b**¹² (2.6 g, 7.6 mmol) in 1 L of CH₂Cl₂ were treated with TCBQ (7.3 g, 30 mmol) and TsOH (1.52 g, 8.0 mmol) as described to give 0.80 g (13%) of **14** as a purple solid; mp > 300 °C. ¹H NMR (500 MHz, CDCl₃): δ 4.11 (s, 6H), 7.40 (AA', 4H, *J* = 8 Hz), 7.86 (m, 6H), 8.25 (BB', 4H, *J* = 8 Hz), 8.32 (d, 4H, *J* = 5 Hz), 8.86 (s, 2H), 8.89 (d, 2H, *J* = 2 Hz), 9.91 (s, 2H), 9.95 (s, 2H). ¹³C NMR (75 MHz, CDCl₃): δ 55.73, 113.35, 127.68, 128.12, 133.64, 134.50, 134.70, 135.85, 137.05, 137.33, 137.63, 141.17, 149.66, 150.35, 156.84, 156.94, 159.96. High-resolution Q-TOF MS: *m/z* 805.0907 (calcd for C₄₆H₃₂N₂O₂Se₂ + H, 805.0878).

Preparation of 5,10,15-Tri(4-methoxyphenyl)-20-phenyl-21,23-dithiaporphyrin (27). Compounds **10**^{12b} (2.39 g, 5.3 mmol) and **23** (1.7 g, 5.2 mmol) were treated with TCBQ (5.4 g, 22 mmol) and TsOH (0.76 g, 4.0 mmol) as described to give 0.72 g (19%) of **27** as a purple solid; mp > 300 °C. ¹H NMR (400 MHz, CDCl₃): δ 4.11 (s, 9H), 7.36 (d, 6H, *J* = 8.0 Hz), 7.81 (m, 3H), 8.18 (d, 6H, *J* = 7.2 Hz), 8.25 (m, 2H), 8.67 (d, 1H, *J* = 4.4 Hz), 8.70 (s, 3H), 9.66 (d, 1H, *J* = 5.2 Hz), 9.71 (s, 3H). ¹³C NMR (75 MHz, CDCl₃): δ 55.74, 113.18, 127.54, 128.11, 133.90, 134.32, 134.53, 134.63, 135.34, 135.55, 141.51, 147.88, 148.14, 148.29, 156.43, 156.71, 156.85, 159.88. High-resolution Q-TOF MS: *m/z* 739.2038 (calcd for C₄₇H₃₄N₂O₃S₂ + H, 739.2089).

General Procedure for Demethylation of Core-Modified Porphyrins 12–14, 24, and 27. Preparation of **5,10,15,20-Tetra(4-hydroxyphenyl)-21,23-dithiaporphyrin (16).** Compounds **8a**^{12b} (1.75 g, 4.9 mmol) and **10** (2.25 g, 5.0 mmol) were treated with TCBQ (2.25 g, 22 mmol) and TsOH (0.95 g, 5.0 mmol) as described. The porphyrin product displayed minimal solubility. The crude product was washed with acetone to give 0.74 g (20%) of **13** as a purple solid; mp 280–282 °C. High-resolution Q-TOF MS: *m/z* 769.2180 (calcd for C₄₈H₃₆N₂O₄S₂ + H, 769.2195). This particular porphyrin was too insoluble for NMR studies and was characterized following demethylation in the next step.

Core-modified porphyrin **13** (0.77 g, 1.0 mmol) was dissolved in CH₂Cl₂ (100 mL), and BBr₃ (0.49 mL, 5.1 mmol) was added at 0 °C. The resulting solution was stirred for 5 h at ambient temperature. The reaction mixture was added to 200 mL of EtOAc and 200 mL of saturated NaHCO₃. The organic layer was separated and washed three times with brine, dried over MgSO₄, and concentrated. The crude solid was washed with 3/1 EtOAc/hexanes several times to give 0.60 g (84%) of **16** as a dark blue solid; mp > 300 °C. ¹H NMR (400 MHz, DMSO-*d*₆): δ 7.26 (AA', 8H, *J* = 7.6 Hz), 7.95 (BB', 8H, *J* = 8.0 Hz), 8.47 (s, 4H), 9.65 (s, 4H). ¹³C NMR (75 MHz, DMSO-*d*₆): δ 115.44, 131.48, 134.38, 134.57, 136.14, 147.47, 155.81, 158.23. High-resolution Q-TOF MS: *m/z* 713.1542 (calcd for C₄₄H₂₈N₂O₄S₂ + H, 713.1569).

Preparation of 5-(4-Hydroxyphenyl)-10,15,20-triphenyl-21,23-dithiaporphyrin (25). Core-modified porphyrin **24** (0.35 g, 0.52 mmol) in 50 mL of CH₂Cl₂ was treated with BBr₃ (0.49 mL, 5.1 mmol) as described for the preparation of **16** to give 0.30 g (87%) of **25** as a purple solid; mp > 300 °C. ¹H NMR (400 MHz, 1:1 CD₃OD/CDCl₃): δ 7.11 (AA', 2H, *J* = 8.4 Hz, 2 × HOCC_H), 7.63 (m, 9H), 7.91 (BB', 2H, *J* = 8.4 Hz), 8.07 (m, 6H), 8.49 (d, 3H, *J* = 4.4 Hz), 8.56 (d, 1H, *J* = 4.4 Hz), 9.52 (d, 3H, *J* = 6.8 Hz), 9.61 (d, 1H, *J* = 4.8 Hz). ¹³C NMR (75 MHz, 1:1 CD₃OD/CDCl₃): δ 114.40, 127.28, 127.94, 132.24, 133.68, 133.85, 133.95, 134.10, 134.21, 134.33, 134.46, 134.70, 135.24, 135.36, 135.46, 135.64, 140.94, 148.34, 147.57,

147.67, 147.95, 156.16, 156.38, 156.76, 157.24. High-resolution Q-TOF MS: *m/z* 665.1708 (calcd for C₄₄H₂₈N₂O₂S₂ + H, 665.1721).

Preparation of 5,10-Bis(4-hydroxyphenyl)-15,20-Diphenyl-21,23-dithiaporphyrin (15). Dithiaporphyrin **12** (312 mg, 0.44 mmol) was treated with BBr₃ (0.78 mL, 8.0 mmol) as described to give 170 mg (57%) of the phenolic dithiaporphyrin **15**, which was recrystallized from CH₂Cl₂/toluene to give purple needles, mp > 300 °C. ¹H NMR (300 MHz, DMSO-*d*₆): δ 10.14 (br s, 2H), 9.78 (s, 2H), 9.66 (s, 2H), 8.67 (d, 2H, *J* = 4.4 Hz), 8.57 (d, 2H, *J* = 4.4 Hz), 8.22 (m, 4H), 8.06 (AA', 4H, *J* = 8.2 Hz), 7.86 (m, 6H), 7.28 (BB', 4H, *J* = 8.2 Hz). ¹³C NMR (75 MHz, DMSO-*d*₆): δ 157.89, 155.82, 155.45, 147.38, 146.60, 140.34, 136.02, 135.67, 135.53, 134.84, 134.62, 134.24, 133.86, 133.40, 130.93, 128.33, 127.76. High-resolution Q-TOF MS: *m/z* 717.1475 (calcd for C₄₄H₂₈N₂O₂S₂ + H, 717.1482).

Preparation of 5,10-Bis(4-hydroxyphenyl)-15,20-Diphenyl-21,23-diselenaporphyrin (17). Diselenaporphyrin **14** (0.40 g, 0.50 mmol) was treated with BBr₃ (0.49 mL, 5.1 mmol) as described to give 0.37 g (96%) of **17** as a purple solid; mp > 300 °C. ¹H NMR (500 MHz, 1:1:1 CDCl₃/CD₃OD/DMSO-*d*₆): δ 7.24 (AA', 4H, *J* = 8 Hz), 7.75 (m, 6H), 8.02 (d, 4H, *J* = 6 Hz), 8.15 (BB', 4H, *J* = 8 Hz), 8.68 (d, 2H, *J* = 4 Hz), 8.76 (d, 2H, *J* = 4 Hz), 9.77 (s, 2H), 9.87 (s, 2H). ¹³C NMR (126 MHz, 1:1:1 CDCl₃/CD₃OD/DMSO-*d*₆): δ 115.04, 127.84, 128.34, 131.93, 134.26, 134.38, 134.84, 136.11, 137.12, 137.17, 137.37, 138.37, 140.74, 149.12, 150.20, 156.61, 156.74, 157.98. High-resolution Q-TOF MS: *m/z* 777.0553 (calcd for C₄₄H₂₈N₂O₂Se₂ + H, 777.0565).

Preparation of 5,10,15-Tris(4-hydroxyphenyl)-20-Phenyl-21,23-dithiaporphyrin (28). Core-modified porphyrin **27** (0.49 g, 0.66 mmol) was treated with BBr₃ (0.49 g, 5.1 mmol) as described to give 0.38 g (82%) of **28** as a purple solid; mp > 300 °C. ¹H NMR (400 MHz, 1:1 CD₃OD/CDCl₃): δ 7.07 (AA', 6H, *J* = 7.6 Hz), 8.09 (m, 3H), 7.83 (BB', 6H, *J* = 7.6 Hz), 7.98 (m, 2H), 8.40 (d, 1H, *J* = 4.4 Hz), 8.44 (s, 2H), 8.47 (d, 1H, *J* = 4.4 Hz), 9.42 (d, 1H, *J* = 5.2 Hz), 9.51 (d, 3H, *J* = 5.2 Hz). ¹³C NMR (75 MHz, 1:1 CD₃OD/CDCl₃): δ 114.33, 127.20, 127.84, 132.15, 133.29, 133.87, 134.07, 135.00, 135.43, 140.83, 147.23, 147.52, 147.66, 147.85, 155.89, 156.45, 157.20. High-resolution Q-TOF MS: *m/z* 697.1624 (calcd for C₄₄H₂₈N₂O₃S₂ + H, 697.1619).

General Procedure for the Preparation of Ethyl Carboxylatomethoxy Core-Modified Porphyrins. Preparation of Ethyl 5,10,15-Triphenyl-20-(4-carboxylatomethoxy)phenyl-21,23-dithiaporphyrin (26). Core-modified porphyrin **25** (0.25 g, 0.38 mmol), 2.6 g of K₂CO₃, and 2.1 mL of ethyl bromoacetate in 60 mL of acetone were heated at reflux for 15 h. The reaction mixture was cooled to ambient temperature, and the K₂CO₃ was removed by filtration. The filter cake was washed with acetone until the filtrate was colorless. The combined filtrates were concentrated. The crude product was washed with MeOH to give 0.22 g (78%) of **26** as a purple solid; mp > 300 °C. ¹H NMR (500 MHz, CDCl₃): δ 1.40 (t, 3H, *J* = 7.0 Hz), 4.42 (q, 2H, *J* = 7.0 Hz), 4.92 (s, 2H), 7.36 (AA', 2H, *J* = 8.5 Hz), 7.81 (br s, 9H), 8.18 (BB', 2H, *J* = 8.5 Hz), 8.26 (m, 6H), 8.69 (m, 4H), 9.69 (m, 4H). ¹³C NMR (75 MHz, CDCl₃): δ 14.43, 61.73, 65.92, 113.94, 127.57, 128.18, 133.79, 134.32, 134.65, 134.89, 135.53, 141.41, 147.92, 148.02, 148.17, 156.54, 156.64, 156.79, 158.24, 169.13. High-resolution Q-TOF MS: *m/z* 751.2065 (calcd for C₄₈H₃₄N₂O₃S₂ + H, 751.2089).

Preparation of Diethyl 5,10-Diphenyl-15,20-bis(4-carboxylatomethoxy)phenyl-21,23-dithiaporphyrin (18). Core-modified porphyrin **15** (126 mg, 0.185 mmol), 1.5 g of K₂CO₃, and 2 mL of ethyl bromoacetate in 50 mL of acetone were treated as described for the preparation of **29** to give 94 mg (60%) of **18** as a purple solid; mp 255–257 °C. ¹H NMR (300 MHz, CDCl₃): δ 9.70 (s, 2H), 9.67 (s, 2H), 8.68 (m, 4H), 8.63 (d, 2H, *J* = 4.5 Hz), 8.22–8.27 (m, 4H), 8.18 (AA', 4H, *J* = 8.4 Hz), 7.77–7.85 (m, 6H), 7.37 (BB', 4H, *J* = 8.4 Hz), 4.93 (s, 4H), 4.42 (q, 4H, *J* = 7.2 Hz), 1.42 (t, 6H, *J* = 7.2 Hz). ¹³C NMR (75 MHz, CDCl₃): δ 168.99, 158.08, 156.57, 156.42, 148.03, 147.76, 141.25, 135.38, 134.74, 134.48, 134.16, 133.93,

133.57, 128.01, 127.41, 113.78, 65.77, 61.59, 14.29. High-resolution Q-TOF MS: m/z 751.2084 (calcd for $C_{52}H_{40}N_2O_6S_2 + H$, 751.2089).

Preparation of Triethyl 5-Phenyl-10,15,20-Tris-(4-carboxylatomethoxy)phenyl-21,23-dithiaporphyrin (29). Core-modified porphyrin **28** (0.30 g, 0.43 mmol) was treated with 2.0 mL of ethyl bromoacetate as described to give 0.38 g (92%) of **29** as a purple solid; mp 182–184 °C. 1H NMR (500 MHz, $CDCl_3$): δ 1.43 (d, 9H, $J = 7.0$ Hz), 4.43 (q, 6H, $J = 7.0$ Hz), 4.92 (s, 6H), 7.36 (d, 6H, $J = 8.0$ Hz), 7.82 (m, 3H), 8.18 (d, 6H, $J = 8.0$ Hz), 8.25 (m, 2H), 8.69 (m, 4H), 9.69 (m, 4H). ^{13}C NMR (75 MHz, $CDCl_3$): δ 14.40, 61.69, 65.84, 113.90, 127.54, 128.14, 133.61, 133.65, 133.71, 134.04, 134.29, 134.61, 134.84, 135.49, 141.37, 147.92, 148.07, 148.18, 156.51, 156.66, 156.76, 158.17, 169.11. High-resolution Q-TOF MS: m/z 955.2726 (calcd for $C_{56}H_{46}N_2O_9S_2 + H$, 955.2723).

Preparation of Tetraethyl 5,10,15,20-Tetra-(4-carboxylatomethoxy)phenyl-21,23-dithiaporphyrin (19). Core-modified porphyrin **16** (0.35 g, 0.49 mmol) was treated with 2 mL of ethyl bromoacetate as described to give 0.30 g (58%) of **19** as a purple solid; mp 146–148 °C. 1H NMR (500 MHz, $CDCl_3$): δ 1.43 (t, 12 H, $J = 7.5$ Hz), 4.43 (q, 8 H, $J = 7.5$ Hz), 4.92 (s, 8 H), 7.36 (AA', 8 H, $J = 8.5$ Hz), 8.18 (BB', 8 H, $J = 8.5$ Hz), 8.69 (s, 4 H), 9.69 (s, 4 H). ^{13}C NMR (75 MHz, $CDCl_3$): δ 14.43, 61.85, 65.95, 113.99, 133.69, 134.70, 134.95, 135.58, 135.64, 148.17, 156.78, 158.25, 169.24. High-resolution Q-TOF MS: m/z 1057.3035 (calcd for $C_{60}H_{52}N_2O_{12}S_2 + H$, 1057.3040).

General Procedure for Saponification of Ethyl Esters of Core-Modified Porphyrins. Preparation of 5,10,15-Triphenyl-20-(4-carboxylatomethoxy)phenyl-21,23-dithiaporphyrin (1). Core-modified porphyrin **26** (0.18 g, 0.24 mmol) was dissolved in 50 mL of THF, and 1 M NaOH (20 mL, 20 mmol) was added. The resulting solution was stirred at ambient temperature for 15 h. The solution was acidified by the addition of 8 mL of acetic acid. The reaction mixture was diluted with 100 mL of H_2O , and the products were extracted with EtOAc (3×100 mL). The combined organic extracts were dried over $MgSO_4$ and concentrated. The crude product was washed with several portions of hexanes/MeOH to give 0.16 g (92%) of **1** as a purple solid; mp 265–267 °C. 1H NMR (500 MHz, $CDCl_3$): δ 5.00 (s, 2H), 7.40 (AA', 2H, $J = 8.0$ Hz), 7.81 (m, 9H), 8.20 (BB', 2H, $J = 8.0$ Hz), 8.24 (m, 6H), 8.68 (s, 4H), 9.68 (d, 4H, $J = 5.0$ Hz). ^{13}C NMR (75 MHz, $CDCl_3$): δ 65.35, 114.00, 127.60, 128.23, 133.56, 134.20, 134.24, 134.36, 134.52, 134.63, 134.71, 135.21, 135.55, 135.64, 135.68, 141.31, 147.93, 147.97, 148.14, 156.37, 156.52, 156.56, 156.60, 157.83, 172.71. High-resolution Q-TOF MS: m/z 723.1761 (calcd for $C_{46}H_{30}N_2O_3S_2 + H$, 723.1776). Anal. C, H, N.

Preparation of 5,10-Diphenyl-15,20-Bis-(4-carboxylatomethoxy)phenyl-21,23-dithiaporphyrin (2). Core-modified porphyrin **18** (55.3 mg, 0.0694 mmol) in 30 mL of THF was treated with 1.46 mL (0.146 mmol) of 0.10 M aqueous NaOH as described to give 52 mg (91%) of core-modified porphyrin **2**; mp > 300 °C. 1H NMR (300 MHz, CD_3OD): δ 9.72 (s, 2 H), 9.60 (s, 2 H), 8.61 (d, 2 H, $J = 4.5$ Hz), 8.53 (d, 2 H, $J = 4.5$ Hz), 8.10–8.17 (m, 4 H), 8.06 (d, 4 H, $J = 8.1$ Hz), 7.74–7.80 (m, 6 H), 7.37 (d, 4 H, $J = 8.1$ Hz), 4.62 (s, 4 H). ^{13}C NMR (75 MHz, CD_3OD): δ 176.51, 160.72, 158.13, 157.76, 149.46, 148.81, 142.39, 136.87, 136.46, 135.82, 135.64, 135.19, 135.10, 134.56, 129.37, 128.69, 115.13, 68.78. High-resolution Q-TOF MS: m/z 841.1427 (calcd for $C_{48}H_{30}N_2Na_2O_6S_2 + H$, 841.1419). Anal. C, H, N.

Preparation of 5-Phenyl-10,15,20-Tris-(4-carboxylatomethoxy)phenyl-21,23-dithiaporphyrin (3). Core-modified porphyrin **29** (0.30 g, 0.31 mmol) in 30 mL of THF was treated with 3 mL (3 mmol) of 1.0 M aqueous NaOH as described to give 0.25 g (91%) of core-modified porphyrin **3** as a purple solid; mp 210–212 °C. 1H NMR (400 MHz, 1:1 $CD_3OD/CDCl_3$): δ 4.96 (s, 6H), 7.44 (AA', 4H, $J = 7.6$ Hz), 7.42 (AA', 2 H, $J = 7.6$ Hz), 7.85 (m, 3H), 8.21 (BB', 6H, $J = 7.6$ Hz), 8.23 (BB', 2 H, $J = 7.6$ Hz), 8.26 (m, 2 H), 8.71 (m, 4H), 9.74 (m, 4H). ^{13}C NMR (75 MHz, 1:1 $CD_3OD/CDCl_3$): δ 65.21, 114.37, 128.28, 133.39, 134.15, 134.31, 135.10, 135.70, 136.31, 140.58, 147.25, 147.45, 147.60, 155.92, 156.14, 156.28, 158.42, 170.85. High-

resolution Q-TOF MS: m/z 871.1750 (calcd for $C_{50}H_{34}N_2O_9S_2 + H$, 871.1784). Anal. C, H, N.

Preparation of 5,10,15,20-Tetra-(4-carboxylatomethoxy)phenyl-21,23-dithiaporphyrin (4). Core-modified porphyrin **19** (0.18 g, 0.17 mmol) in 20 mL of THF was treated with 2 mL (2 mmol) of 1 M NaOH as described to give 0.11 g (68%) of core-modified porphyrin **4**; mp 212–214 °C. 1H NMR (500 MHz, 1:1 $CD_3OD/CDCl_3$): δ 4.92 (s, 8 H), 7.40 (AA', 8 H, $J = 8.0$ Hz), 8.14 (BB', 8 H, $J = 8.0$ Hz), 8.64 (s, 4 H), 9.70 (s, 4 H). ^{13}C NMR (126 MHz, 1:1 $CD_3OD/CDCl_3$): δ 64.15, 67.93, 112.82, 126.60, 132.62, 133.19, 133.24, 134.11, 134.31, 147.19, 148.24, 155.57, 157.70, 167.07, 168.82. High-resolution Q-TOF MS: m/z 945.1807 (calcd for $C_{52}H_{36}N_2O_{12}S_2 + H$, 945.1788). Anal. C, H, N.

Preparation of 5,10-Diphenyl-15,20-Bis-(4-carboxylatomethoxy)phenyl-21,23-diselenaporphyrin (5). Core-modified porphyrin **20** (0.28 g, 0.30 mmol) in 30 mL of THF was treated with 3 mL (3 mmol) of 1.0 M aqueous NaOH as described to give 0.25 g (95%) of porphyrin **5**; mp 255–257 °C. 1H NMR (500 MHz, 1:1 $CDCl_3/DMSO-d_6$): δ 4.90 (s, 4H), 7.40 (AA', 4H, $J = 8$ Hz), 7.81 (m, 6H), 8.19 (BB', 4H, $J = 8$ Hz), 8.24 (m, 4H), 8.79 (s, 4H), 9.86 (s, 2H), 9.88 (s, 2H). ^{13}C NMR (75 MHz, 1:1 $CDCl_3/DMSO-d_6$): δ 65.40, 113.94, 127.56, 128.06, 134.35, 134.48, 135.68, 137.03, 137.15, 137.36, 140.90, 149.59, 150.05, 156.73, 156.73, 156.78, 158.18, 171.19. High-resolution Q-TOF MS: m/z 893.0654 (calcd for $C_{48}H_{32}N_2O_6^{80}Se_2 + H$, 893.0676). Anal. C, H, N.

Quantum Yield Determinations for the Generation of Singlet Oxygen. The quantum yields for singlet oxygen generation with 21,23-dithiaporphyrin **1–4** were measured by direct methods in MeOH.¹⁶ A SPEX 270M spectrometer (Jobin Yvon) equipped with InGaAs photodetector (Electrooptical Systems Inc., U.S.A.) was used for recording singlet oxygen emission spectra. A diode-pumped solid state laser (Millenia X, Spectra-Physics) at 532 nm was the excitation source. The sample solution in a quartz cuvette was placed directly in front of the entrance slit of the spectrometer, and the emission signal was collected at 90° relative to the exciting laser beam. An additional long-pass filter (850LP) was used to attenuate the excitation laser and the fluorescence from the photosensitizer.

Determination of Partition Coefficients. The octanol/water partition coefficients were all measured at pH 7.4 (PBS) using UV–visible spectrophotometry. The measurements were done using a shake flask direct measurement.¹⁸ Mixing for 3–5 min was followed by 1 h of settling time. Equilibration and measurements were made at 23 °C using a Perkin-Elmer Lambda 12 spectrophotometer. High-performance liquid chromatography grade 1-octanol was obtained from Sigma-Aldrich.

Cells and Culture Conditions. R3230AC Cells. Cells cultured from the rodent mammary adenocarcinoma (R3230AC) were used for these studies. The R3230AC tumors were maintained by transplantation in the abdominal region of 100–120 g Fischer female rats, using the sterile trocar technique described by Hilf et al.²⁹ R3230AC cells were cultured from tumor homogenates using the method described earlier.³⁰ All cell lines were maintained in passage culture on 100 mm diameter polystyrene dishes (Becton Dickinson, Franklin Lakes, NJ) in 10 mL of minimum essential medium (α -MEM) supplemented with 10% FBS, 50 units/mL penicillin G, 50 μ g/mL streptomycin, and 1.0 μ g/mL Fungizone growth media. Only cells from passages 1–10 were used for experiments. Cells, passages 1–4, that were maintained at –86 °C were used to initiate the experimental cultures. Cultures were maintained at 37 °C in a 5% CO_2 humidified atmosphere (Forma Scientific, Marietta, OH). Passage was accomplished by removing the culture medium, and then adding a 1 mL solution containing 0.25% trypsin, incubating at 37 °C for 2–5 min to remove the cells from the surface followed by seeding new culture dishes with an appropriate number of cells in 10 mL of α -MEM. Cell counts were performed using a particle counter (model ZM, Coulter Electronics, Hialeah, FL).

Incubation with Core-Modified Porphyrins 1–5. For experiments designed to determine cell viability in the pres-

ence of individual core-modified porphyrins (1–5) in the dark and after light exposure, R3230AC cells were removed from the 100 mm dishes via trypsinization, see above, and seeded on 12 well plates at $0.5\text{--}0.8 \times 10^5$ cells/well in 1.0 mL of growth media. Cultures were incubated for 24 h, as above, after which the appropriate concentrations of 1–5 were added directly to the wells in the growth medium. Cells were then incubated with the core-modified porphyrins for selected times.

For experiments designed to determine the amount of intracellular porphyrin after 3 or 24 h incubation periods in the presence of core-modified porphyrins, cells were seeded on 12 well plates as above, and 24 h after seeding, compounds 1–5 were added at the appropriate concentrations in the growth. Cells were incubated at 37 °C in the dark for either 3 or 24 h when the intracellular porphyrin content was determined.

Measurement of Porphyrin Content in Cultured Cells. Determination of the levels of core-modified porphyrins in cultured cells was performed in 12 well plates using fluorescence. Following the incubation periods in the presence of 1–5, the growth medium was removed, and the cell monolayers were washed once with 1.0 mL of 0.9% saline. Cells in selected wells were detached using a 0.25% trypsin solution, and the number of cells per well was determined using a Coulter counter as described above. The saline wash was removed, and 1.0 mL of Scintigest was added. Porphyrin fluorescence was determined using a multiwell fluorescence plate reader (Molecular Devices, Sunnyvale, CA). Excitation was at 440 nm, and the major fluorescent peak at 725 nm was used to calculate the porphyrin concentration, which was obtained by comparing the fluorescence values (or absorbance values for 5) with measurements from known concentrations of 1–5 in Scintigest. Data are expressed as femtomoles of core-modified porphyrin/cell.

Irradiation of Cultured R3230AC Cells. Following incubation for 3 or 24 h with porphyrins on 12 well plates, the growth medium containing the porphyrins was removed from cell monolayers, cells were washed once with 1.0 mL of 0.9% NaCl and 1.0 mL of medium minus FBS, and phenol red (clear medium) was added. Plates, with lids removed, were positioned on a orbital shaker (LabLine, Melrose Park, IL) and then exposed for various times to broadband light (350–750 nm) delivered at 1.4 mW cm^{-2} from a filtered 750 W tungsten source defocused to encompass the whole 12 well plate. The culture plates were gently orbited on the shaker in order to ensure uniform illumination of all of the wells on the plate. The medium was then removed, and 1.0 mL of fresh growth medium was added and cultures were incubated at 37 °C for 24 h in the dark. Plates were also maintained in the dark and underwent the same changes in cell culture medium as those that were irradiated. These were used to determine the dark toxicity of 1–5 at 24 and 48 h after addition of 1–5 to the monolayers. Cell counts, using the Coulter counter as above, were made on control nonirradiated cells and on irradiated cells or cells maintained in the dark. Previously, when we used trypan blue dye exclusion to determine cell viability, we found that all of the cells that had detached from the surface and were floating in the medium stained with trypan blue, i.e., nonviable, while those cells that remained attached to the surface excluded trypan blue. Culturing of the cells that detached was unsuccessful while passing those cells that remained attached resulted in a plating efficiency similar to that of untreated cells. Therefore, we counted the cells that remained attached to the plate after treatment and used those numbers to determine viability. Data for cell viability are expressed as the percent of control cell counts, cells that were not exposed to either porphyrins or irradiation.

Cells and Culture Conditions. Colo-26 Cells. Colo-26, a murine colon carcinoma cell line, was maintained in a growth medium of RPMI 1640 supplemented with 10% fetal calf serum (FCS) and antibiotics (all components purchased from GIBCO Laboratories) at 37 °C, 5% CO₂.

Irradiation of Cultured Colo-26 Cells. Colo-26 cells were plated at 5×10^3 cells/well of a 96 well tissue culture plate

the evening before the assay. The day of the assay, the cells were washed twice with PBS and 100 μL of Hank's basic salt solution (HBSS) with 1% FCS containing various concentrations of dithiaporphyrins 2 and 30, HPPH, and Photofrin was added to each well. The dye and cells were incubated for 2 h at 37 °C followed by a wash with PBS and the addition of 100 μL of PBS supplemented with 1% FCS. The plates were irradiated with filtered 590–800 nm light at 14 mW cm^{-2} for a total light dose of 4 J cm^{-2} . Following irradiation, 100 μL of growth media was added and the plates were incubated for 24 h at 37 °C, 5% CO₂. Control cells (no dye + light; dye + no light) were treated using the same conditions. Cell survival was monitored using the MTT assay as described by Mosmann.³¹

Photobleaching Conditions. Studies of the rates of photobleaching of core-modified porphyrins 1–5 were carried out in PBS (0.05 M, pH 7.4). Stock solutions of 1–5 and Photofrin (1×10^{-3} M) in clear medium were diluted in PBS. Concentrations ($\approx 5 \times 10^{-6}$ M) were adjusted such that the initial absorbance of the solet band was ≈ 1.0 in a 1 cm cell. Initial absorption was measured using a diode array spectrophotometer (HP8452, Hewlett-Packard, Palo Alto, CA). Irradiation of 1–5 or Photofrin was accomplished by exposing 1.0 mL of 1–5 or Photofrin to 200 mW/cm² broadband 350–750 nm white light emitted from a focused and filtered 750 W tungsten source. Absorption spectra were acquired at selected intervals, and rates of photobleaching were determined by the reduction in the absorption maximum of each compound over time of irradiation.

CLSM Studies. R3230AC cells were grown in a tissue culture flask containing α -MEM medium with phenol red (GIBCO, Rockville, MD) and 10% FBS (GIBCO). Cells were trypsinized from the culture flask and were resuspended in medium at a concentration of 7.5×10^5 cells/mL. Then, in 60 mm culture plates, 5 mL of α -MEM medium was combined with 0.10 mL of cell suspension. The plates were then placed overnight in an incubator at 37 °C with 5% CO₂ (VWR Scientific model 2400, Bridgeport, NJ). The next day, the cells (with about 70% confluence) were rinsed with PBS (GIBCO), and 5 mL of α -MEM medium (without phenol red) containing 1 μM Rh-123 or 2 μM 1 or 2 was replaced in each plate. The plates were returned to the incubator (37 °C, 5% CO₂) for a duration of 3 h for 1 and 2 and 20 min for Rh-123. After incubation, the plates were rinsed with sterile PBS, and fresh media (without phenol red) was replaced at a volume of 5 mL/plate. The plates were then observed directly under the confocal microscope. For costaining experiments, cells were treated as described with 1 or 2 for 3 h, were rinsed once with sterile PBS, and were then treated with 1 μM Rh-123 for 20 min as described.

CLSM images were obtained using a commercial CLSM system, model MRC-1024 (Bio-Rad, Richmond, CA), which was attached onto an upright microscope (Nikon, model Eclipse E800). A water immersion objective lens (Nikon, Fluor-60X, NA = 1.0) was used for cell imaging. A solid state diode-pumped laser (Verdi, Coherent) was used as a source of excitation (532 nm). An additional long-pass filter (585LP) was introduced in front of the photomultiplier to minimize leakage of the excitation light. To confirm that the observed fluorescence was from photosensitizer permeated to cells, we used localized spectrofluorometry. The fluorescence signal was collected from the upper port of the confocal microscope using a multimode optical fiber of core diameter 1 mm and was delivered to a spectrometer (Holospec from Kaiser Optical Systems, Inc.) equipped with a cooled charge coupled device camera (Princeton Instruments) as detector. A comparison of the fluorescence spectra from cells and the fluorescence spectra of the photosensitizers confirmed that the origin of the fluorescence observed in the image channel was from the photosensitizer. Control cells showed no fluorescence under the same imaging conditions in the absence of photosensitizer. A 640 nm short-pass dichroic mirror (Chroma) mounted at a 45° angle to the fluorescence beam was employed in costaining experiments.

Cytochrome *c* Oxidase Measurements in Cultured R3230AC Tumor Cells. To determine whether core-modified porphyrin **2** affected mitochondrial cytochrome *c* oxidase activity, R3230AC cells were plated on 12 well culture plates as described until they reached $4\text{--}7 \times 10^5$ cells/well, a number when the cells were still in log phase growth. The complete medium was removed, and fresh clear medium with core-modified porphyrin **2** at 1×10^{-8} , 1×10^{-7} , and 1×10^{-6} final concentration or without photosensitizer for control cells was added. Cells were then incubated for 24 h in the dark at 37 °C with 5% CO₂, the medium was removed, and the cells were washed once with 0.9% NaCl, and 1.0 mL of clear medium was added. Monolayers were then exposed to filtered, 350–750 nm light from a 750 W tungsten source (1.3 mW cm^{-2}) for 1 h as described above (4.7 J cm^{-2}). Immediately following irradiation, the medium was removed from the substrate and replaced with complete medium. Both irradiated cells and dye-treated dark controls were incubated for 24 h in the dark, and the activity of cytochrome *c* oxidase was determined according to the method described earlier.²⁸ Data are expressed as $\Delta \text{m OD}/\text{min}/10^5$ cells at 550 nm and compared to that determined from cells not exposed to dye or light. Cytochrome *c* oxidase activity was also determined in cells exposed to dye alone or light alone, drug and light controls, respectively.

Statistical Analyses. All statistical analyses were performed using the Student's *t*-test for pairwise comparisons. A *P* value of <0.05 was considered significant.

Acknowledgment. We thank Dr. Haridas Pudavar for helpful assistance and discussions in obtaining the confocal microscopy images. We also thank the National Institutes of Health (Grant CA69155 to M.R.D. and Grant CA36856 to R.H.) and the New York State Department of Health for grants in support of this work.

Supporting Information Available: Figures S1–S5 showing absorption spectra for compounds **1–5**, Figure S6 showing singlet oxygen luminescence following irradiation of **1–4** and **30**, Figure S7 showing absorbance at 532 nm for **1–5** and **30**, Figure S8 showing singlet oxygen luminescence following irradiation of **5**, Figures S9–S13 showing dark toxicity for **1–5**, and Figure S14 showing localized spectrofluorometry from R3230AC cells treated with dithiaporphyrin **1**. This information is available free of charge via the Internet at <http://pubs.acs.org>.

References

- Dougherty, T. J.; Gomer, C. J.; Henderson, B. W.; Jori, G.; Kessel, D.; Korbelik, M.; Moan, J.; Peng, Q. Photodynamic Therapy. *J. Natl. Cancer Inst.* **1998**, *90*, 889–905.
- Henderson, B. W.; Dougherty, T. J. How Does Photodynamic Therapy Work? *Photochem. Photobiol.* **1992**, *55*, 145–157.
- (a) Sharman, W. M.; Allen, C. M.; van Lier, J. E. Photodynamic Therapeutics: Basic Principles and Clinical Applications. *Drug Discovery Today* **1999**, *4*, 507–517. (b) Detty, M. R. Photosensitizers for the Photodynamic Therapy of Cancer and Other Diseases. *Expert Opin. Ther. Pat.* **2001**, *11*, 1849–1860.
- Kato, H. Photodynamic Therapy for Lung Cancer – A Review of 19 Years' Experience. *J. Photochem. Photobiol., B* **1998**, *42*, 96–99.
- Guillemin, F.; Feintrenie, X.; Lignon, D. Photodynamic Therapy of Bronchial Cancers. *Rev. Pneumologie Clin.* **1992**, *48*, 111–114.
- Puolakkainen, P.; Schroder, T. Photodynamic Therapy of Gastrointestinal Tumors: A Review. *Dig. Dis.* **1992**, *10*, 53–60.
- Noske, D. P.; Wolbers, J. G.; Sterenberg, H. J. Photodynamic Therapy of Malignant Glioma. A Review of Literature. *Clin. Neurol. Neurosurg.* **1991**, *93*, 293–307.
- Moesta, K. T.; Schlag, P.; Douglass, H. O., Jr.; Mang, T. S. Evaluating the Role of Photodynamic Therapy in the Management of Pancreatic Cancer. *Lasers Surg. Med.* **1995**, *16*, 84–92.
- Bellnier, D. A.; Dougherty, T. J. A Preliminary Pharmacokinetic Study of Intravenous Photofrin in Patients. *J. Clin. Laser Med. Surg.* **1996**, *14*, 311–314.
- Dougherty, T. J.; Marcus, S. L. Photodynamic Therapy. *Eur. J. Cancer* **1992**, *28A*, 1734–1742.
- (a) Potter, W. R.; Henderson, B. W.; Bellnier, D. A.; Pandey, R. K.; Vaughan, L. A.; Weishaupt, K. R.; Dougherty, T. J. Parabolic Quantitative Structure–Activity Relationships and Photodynamic Therapy: Application of a Three-Component Model with Clearance to the In Vivo Quantitative Structure–Activity Relationships of a Congeneric Series of Porphyrin Derivatives Used as Photosensitizers for Photodynamic Therapy. *Photochem. Photobiol.* **1999**, *70*, 781–788. (b) Sessler, J. L.; Miller, R. A. Texaphyrins—New Drugs with Diverse Clinical Applications in Radiation and Photodynamic Therapy. *Biochem. Pharmacol.* **2000**, *59*, 733–739. (c) Sternberg, E. D.; Dolphin, D.; Brückner, C. Porphyrin-based Photosensitizers for Use in Photodynamic Therapy. *Tetrahedron* **1998**, *54*, 4151–4202. (d) Schmidt, S. Photodynamic Therapy in Breast Cancer Patients: Application of SnET2 for Skin Metastases. *Photomed. Gynecol. Reprod.* **2000**, 316–321. (e) Colussi, V. C.; Feyes, D. K.; Mulvihill, J. W.; Li, Y.-S.; Kenney, M. E.; Elmets, C. A.; Oleinick, N. L.; Mukhtar, H. Phthalocyanine 4(Pc4) Photodynamic Therapy of Human OVCAR-3 Tumor Xenografts. *Photochem. Photobiol.* **1999**, *69*, 236–241. (f) Rovers, J. P.; Saarnak, A. E.; de Jode, M.; Sterenberg, H. J.; Terpstra, O. T. Biodistribution and Bioactivity of Tetra-Pegylated meta-Tetra(hydroxyphenyl)chlorin Compared to Native meta-Tetra(hydroxyphenyl)chlorin in a Rat Liver Tumor Model. *Photochem. Photobiol.* **2000**, *71*, 211–217. (g) Hornung, R.; Fehr, M. K.; Monti-Frayne, J.; Krasieva, T. B.; Tromberg, B. J.; Berns, M. W.; Tadir, Y. Highly Selective Targeting of Ovarian Cancer with the Photosensitizer PEG-mTHPC in a Rat Model. *Photochem. Photobiol.* **1999**, *70*, 624–629. (h) Marcinkowska, E.; Ziolkowski, P.; Pacholska, E.; Latos-Grazynski, L.; Chmielewski, P.; Radzikowski, C. Z. The New Sensitizing Agents for Photodynamic Therapy: 21-Selenaporphyrin and 21-Thiaporphyrin. *Anticancer Res.* **1997**, *17*, 3313–3320.
- (a) Stilts, C. E.; Nelen, M. I.; Hilmey, D. G.; Davies, S. R.; Gollnick, S. O.; Oseroff, A. R.; Gibson, S. L.; Hilf, R.; Detty, M. R. Water-soluble, Core-Modified Porphyrins as Novel, Longer-Wavelength-Absorbing Sensitizers for Photodynamic Therapy. *J. Med. Chem.* **2000**, *43*, 2403–2410. (b) Hilmey, D. G.; Abe, M.; Nelen, M. I.; Stilts, C. E.; Baker, G. A.; Baker, S. N.; Bright, F. V.; Davies, S. R.; Gollnick, S. O.; Oseroff, A. R.; Gibson, S. L.; Hilf, R.; Detty, M. R. Water-soluble, Core-Modified Porphyrins as Novel, Longer-Wavelength-Absorbing Sensitizers for Photodynamic Therapy. II. Effects of Core Heteroatoms and Meso-Substituents on Biological Activity. *J. Med. Chem.* **2002**, *45*, 449–461.
- (a) Ulman, A.; Manassen, J.; Frolow, F.; Rabinovich, D. Synthesis of New Tetrphenylporphyrin Molecules Containing Heteroatoms Other than Nitrogen: II. Tetrphenyl-21-selena-23-thiaporphyrin and Tetrphenyl-21,23-diselenaporphyrin. *Tetrahedron Lett.* **1978**, 167–170. (b) Ulman, A.; Manassen, J.; Frolow, F.; Rabinovich, D. Synthesis of New Tetrphenylporphyrin Molecules Containing Heteroatoms other than Nitrogen. III. Tetrphenyl-21-tellura-23-thiaporphyrin: An Internally-Bridged Porphyrin. *Tetrahedron Lett.* **1978**, 1885–1886.
- Latos-Grazynski, L.; Lisowski, J.; Olmstead, M. M.; Balch, A. L. Five-Coordinate Complexes of 21-Thiaporphyrin. The Preparation, Spectra and Structures of Iron(II), Nickel(II), and Copper(II) Complexes. *Inorg. Chem.* **1989**, *28*, 1183–1188.
- Struharik, M.; Toma, S. The Diastereoselectivity of The Addition of Tricarbonyl-(2-lithiothiophene) Chromium(0) Complexes on Aldehydes. *J. Organomet. Chem.* **1994**, *464*, 59–63.
- Pandey, R. K.; Sumlin, A. B.; Constantine, S.; Aoudia, M.; Potter, W. R.; Bellnier, D. A.; Henderson, B. W.; Rodgers, M. A.; Smith, K. M.; Dougherty, T. J. Alkyl Ether Analogues of Chlorophyll-a Derivatives: Part 1. Synthesis, Photophysical Properties and Photodynamic Efficacy. *Photochem. Photobiol.* **1996**, *64*, 194–204.
- Sangster, J. In *Octanol–Water Partition Coefficients: Fundamentals and Physical Chemistry*; Wiley Series in Solution Chemistry; Fogg, P. G. T., Ed.; John Wiley and Sons: New York, 1997.
- Brennan, N. K.; Hall, J. P.; Davies, S. R.; Gollnick, S. O.; Oseroff, A. R.; Gibson, S. L.; Hilf, R.; Detty, M. R. In Vitro Photodynamic Properties of Chalcogenopyrylium Analogues of the Thiopyrylium Antitumor Agent AA1. *J. Med. Chem.* **2002**, *45*, 5123–5135.
- (a) Krämer, S. D. Absorption Prediction from Physicochemical Parameters. *Pharm. Sci. Technol. Today* **1999**, *2*, 373–380. (b) Beresford, A. P.; Selick, H. E.; Tarbit, M. H. The Emerging Importance of Predictive ADME Simulation in Drug Discovery. *Drug Discovery Today* **2002**, *7*, 109–116.
- Oleinick, N. L.; Evans, H. H. The Photobiology of Photodynamic Therapy: Cellular Targets and Mechanisms. *Radiat. Res.* **1998**, *150* (Suppl.), S146–S156.
- Wikstrom, M.; Krab, K.; Saraste, M. In *Cytochrome Oxidase—A Synthesis*; Academic: New York, 1981.
- Millish, K. J.; Cox, R. D.; Vernon, D. I.; Griffiths, J.; Brown, S. B. In Vitro Photodynamic Activity of a Series of Methylene Blue Analogues. *Photochem. Photobiol.* **2002**, *75*, 392–397.
- (a) Trivedi, N. S.; Wang, h.-W.; Nieminen, a.-L.; Oleinick, N. L.; Izatt, J. A. Quantitative Analysis of Pc 4 Localization in Mouse Lymphoma (LY-R) Cells via Double-label Confocal Fluorescence Microscopy. *Photochem. Photobiol.* **2000**, *71*, 634–639. (b) Mac-

- Donald, I. J.; Morgan, J.; Bellnier, D. A.; Paszkiewicz, G. M.; Whitaker, J. E.; Litchfield, D. J.; Dougherty, T. J. Subcellular Localization Patterns and Their Relationship to Photodynamic Activity of Pyropheophorbid-*a* Derivatives. *Photochem. Photobiol.* **1999**, *70*, 789–797.
- (24) Johnson, L. V.; Walsh, M. L.; Chen, L. B. Localization of Mitochondria in Living Cells with Rhodamine 123. *Proc. Natl. Acad. Sci. U.S.A.* **1980**, *77*, 990–994.
- (25) (a) Kessel, D.; Thompson, P.; Saatio, K.; Nantwi, K. D. Tumor Localization and Photosensitization by Sulfonated Derivatives of Tetraphenylporphine. *Photochem. Photobiol.* **1987**, *45*, 787–790. (b) Kessel, D.; Woodburn, K. Biodistribution of Photosensitizing Agents. *Int. J. Biochem.* **1993**, *25*, 1377–1383. (c) Meng, G. G.; James, B. R.; Skov, K. A.; Korbek, M. Porphyrin Chemistry Pertaining to the Design of Anti-cancer Drugs; Part 2, the Synthesis and in Vitro Tests of Water-soluble Porphyrins Containing in the *meso* Positions, the Functional Groups: 4-Methylpyridinium, 4-Sulfonatophenyl, in Combination with Phenyl, 4-Pyridyl, 4-Nitrophenyl, or 4-Aminophenyl. *Can. J. Chem.* **1994**, *71*, 2447–2457.
- (26) (a) Verma, A.; Nye, J. S.; Snyder, S. H. Porphyrins are Endogenous Ligands for the Mitochondrial (peripheral-tyr) Benzodiazepine Receptor. *Proc. Natl. Acad. Sci. U.S.A.* **1987**, *84*, 2256–2260. (b) Varma, A.; Snyder, S. H. Characterization of Porphyrin Interactions with Peripheral Type Benzodiazepine Receptors. *Mol. Pharmacol.* **1988**, *34*, 800–805. (c) Varma, A.; Fachina, S. L.; Hirsch, D. J.; Song, S. Y.; Dillahey, L. F.; Williams, J. R.; Snyder, S. H. *Mol. Med.* **1998**, *4*, 40–45.
- (27) (a) Kim, H. R.; Luo, Y.; Li, G.; Kessel, D. Enhanced Apoptotic Response to Photodynamic Therapy after Bcl-2 transfection. *Cancer Res.* **1999**, *59*, 3429–3432. (b) Xue, L. Y.; Chiu, S. M.; Oleinick, N. L. Photochemical Destruction of the Bcl-2 Onco-protein During Photodynamic Therapy with the Phthalocyanine Photosensitizer Pc 4. *Oncogene* **2001**, *20*, 3420–3427.
- (28) (a) Kessel, D.; Antolovich, M.; Smith, K. M. The Role of the Peripheral Benzodiazepine Receptor in the Apoptotic Response to Photodynamic Therapy. *Photochem. Photobiol.* **2001**, *74*, 346–349. (b) Morris, L.; Varnes, M. E.; Kenney, M. E.; Li, Y.-S.; Azizuddin, K.; McEnery, M. W.; Oleinick, N. L. The Peripheral Benzodiazepine Receptor in Photodynamic Therapy with the Phthalocyanine Photosensitizer Pc 4. *Photochem. Photobiol.* **2002**, *75*, 652–661.
- (29) Hilf, R.; Michel, I.; Bell, C.; Freeman, J. J.; Borman, A. Biochemical and Morphological Properties of a New Lactating Tumor Line in the Rat. *Cancer Res.* **1965**, *25*, 286–299.
- (30) Hissin, P. J.; Hilf, R. Effects of Insulin in Vivo and in Vitro on Amino Acid Transport into Cells from R3230AC Mammary Adenocarcinoma and Their Relationship to Tumor Growth. *Cancer Res.* **1978**, *38*, 3646–3651.
- (31) Mosmann, T. Rapid Colorimetric Assay for Cellular Growth and Survival: Application to Proliferation and Cytotoxicity Assays. *J. Immunol. Methods* **1983**, *65*, 55–63.

JM030136I